2005/09/23 Oulu, Finland

UWB Double-Directional Channel Sounding

- Why and how? -

Jun-ichi Takada

Tokyo Institute of Technology, Japan

takada@ide.titech.ac.jp

Table of Contents

- Background and motivation
- Antennas and propagation in UWB
- UWB double directional channel sounding system
- Parametric multipath modeling for UWB
- ML-based parameter estimation
- Examples

UWB Systems

- Low power
  - Short range
- Location awareness
  - High resolution in time domain
- Example applications
  - IEEE 802.15.3a : high speed PAN
  - IEEE 802.15.4a : low speed and location aware
  - Ground penetrating radar

Impulse radio

– Simple hardware

– Low power consumption

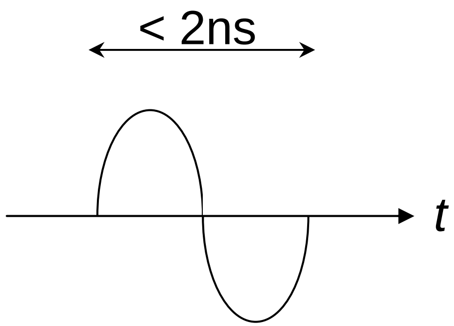

Indoor Multipath Environment

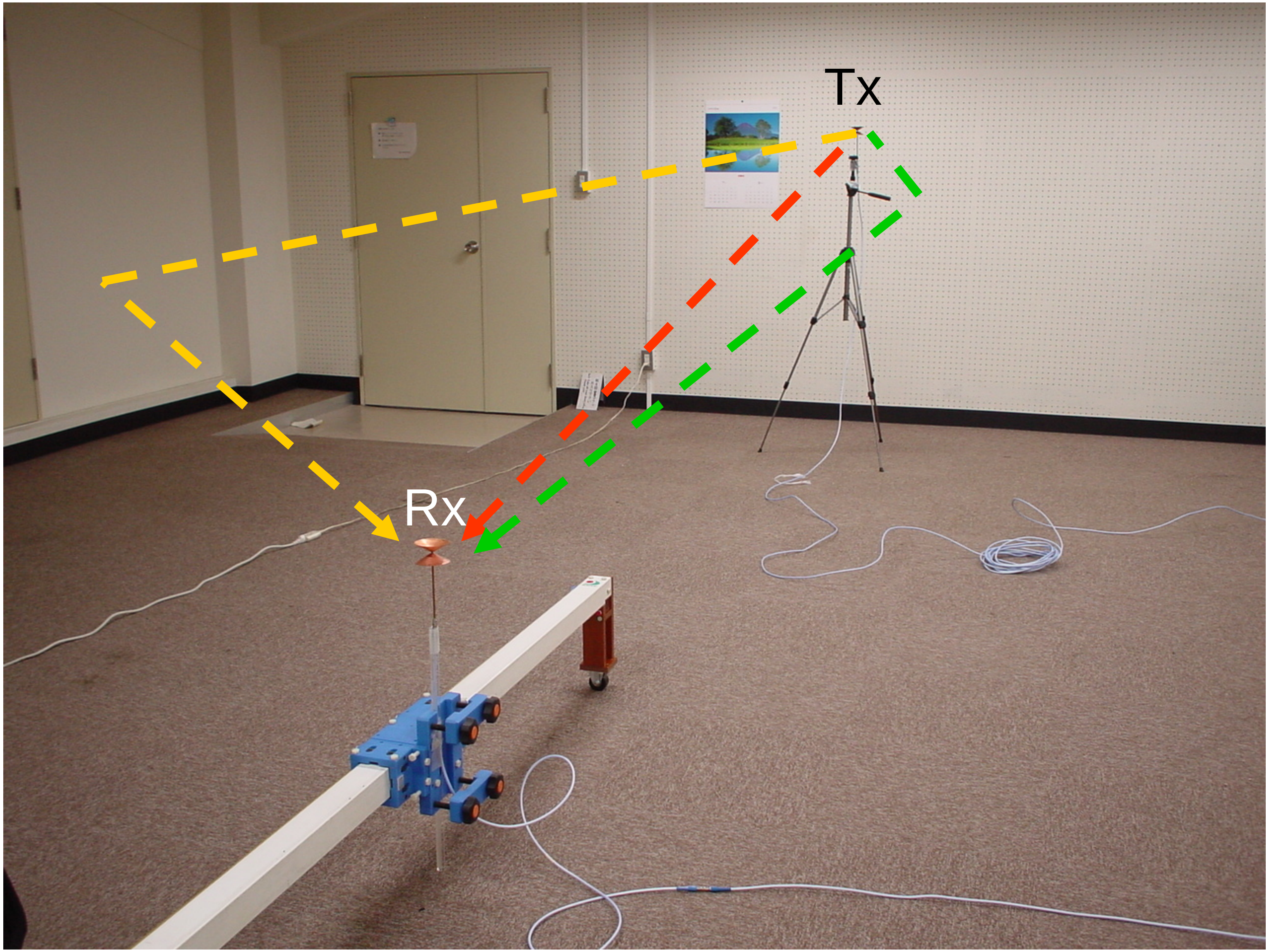

Transmission in Multipath Environment

Tx pulse (500MHz BW)

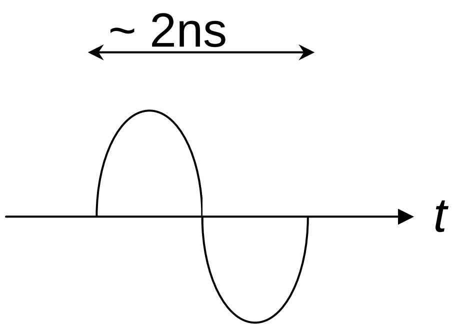

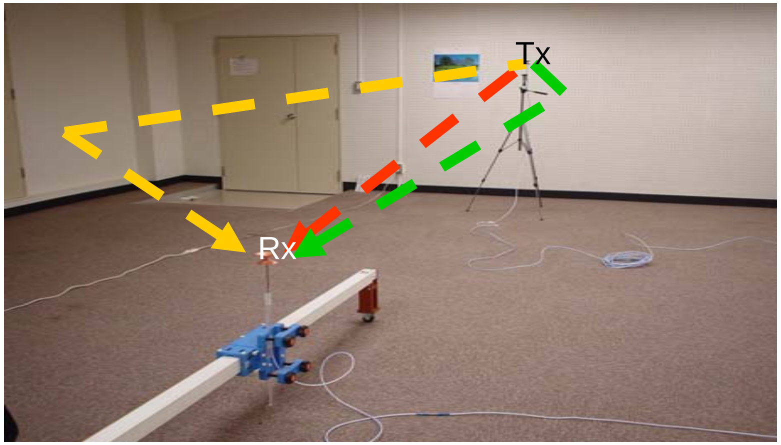

Rx pulse

Multipath components can be distinct

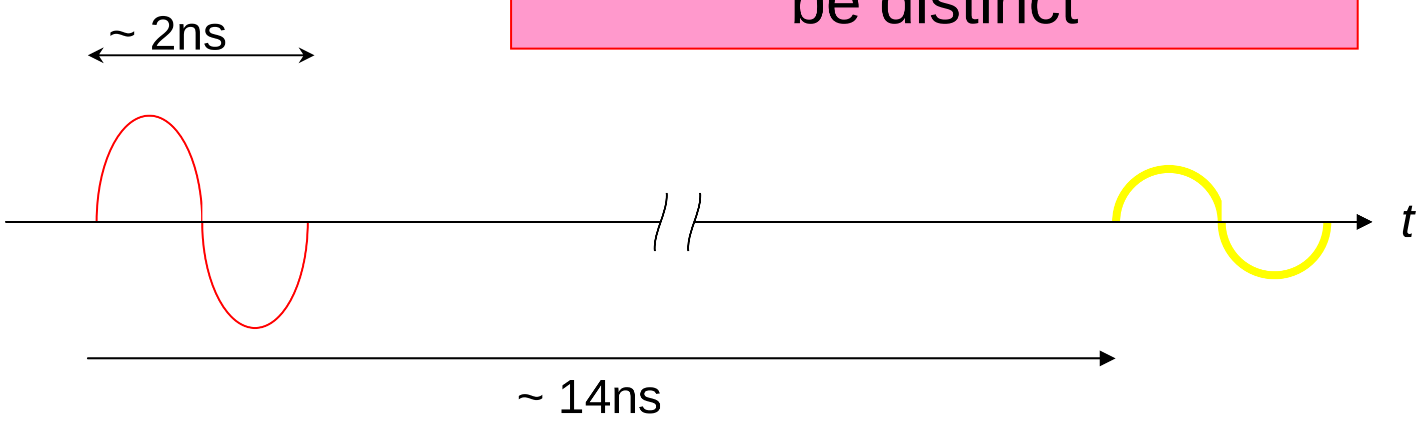

Free Space Transfer Function

- Friis' transmission formula

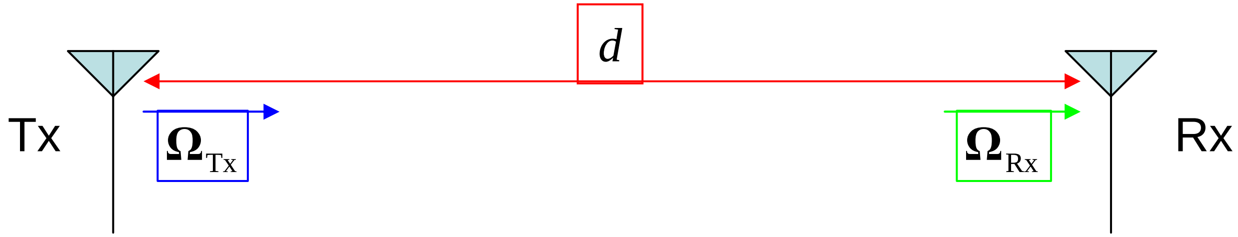

$$H_{\mathrm{Friis}}(f) = H_{\mathrm{Free\,Space}}(f,d)\,\mathbf{H}_{\mathrm{Tx}}(f,\mathbf{\Omega}_{\mathrm{Tx}}) \cdot \mathbf{H}_{\mathrm{Rx}}(f,\mathbf{\Omega}_{\mathrm{Rx}})$$

$$H_{\mathrm{Free\,Space}}(f,d) \propto \frac{1}{f}$$

$\mathbf{H}_{\mathrm{Tx}}(f,\mathbf{\Omega}_{\mathrm{Tx}}) \cdot \mathbf{H}_{\mathrm{Rx}}(f,\mathbf{\Omega}_{\mathrm{Rx}})$: Normalized by isotropic antenna

Ideal Antenna Cases

- Constant aperture size

Example : Pyramidal horn

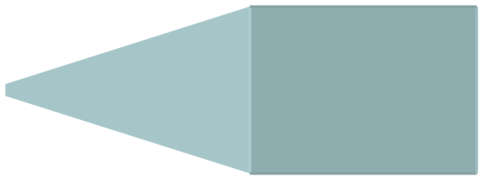

$$H_{\text{Ant}} \dot{\propto} f$$

$$\rightarrow \quad H_{\text{Friis}} \dot{\propto} f$$

- Constant gain

Example : Biconical

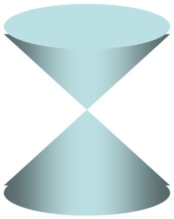

$$H_{\text{Ant}} \doteq \text{const.}$$

$$\rightarrow \quad H_{\text{Friis}} \dot{\propto} \frac{1}{f}$$

Both are too idealized

Frequency Characteristics of Antenna

4.8cm Dipole (resonant at 3.1GHz)

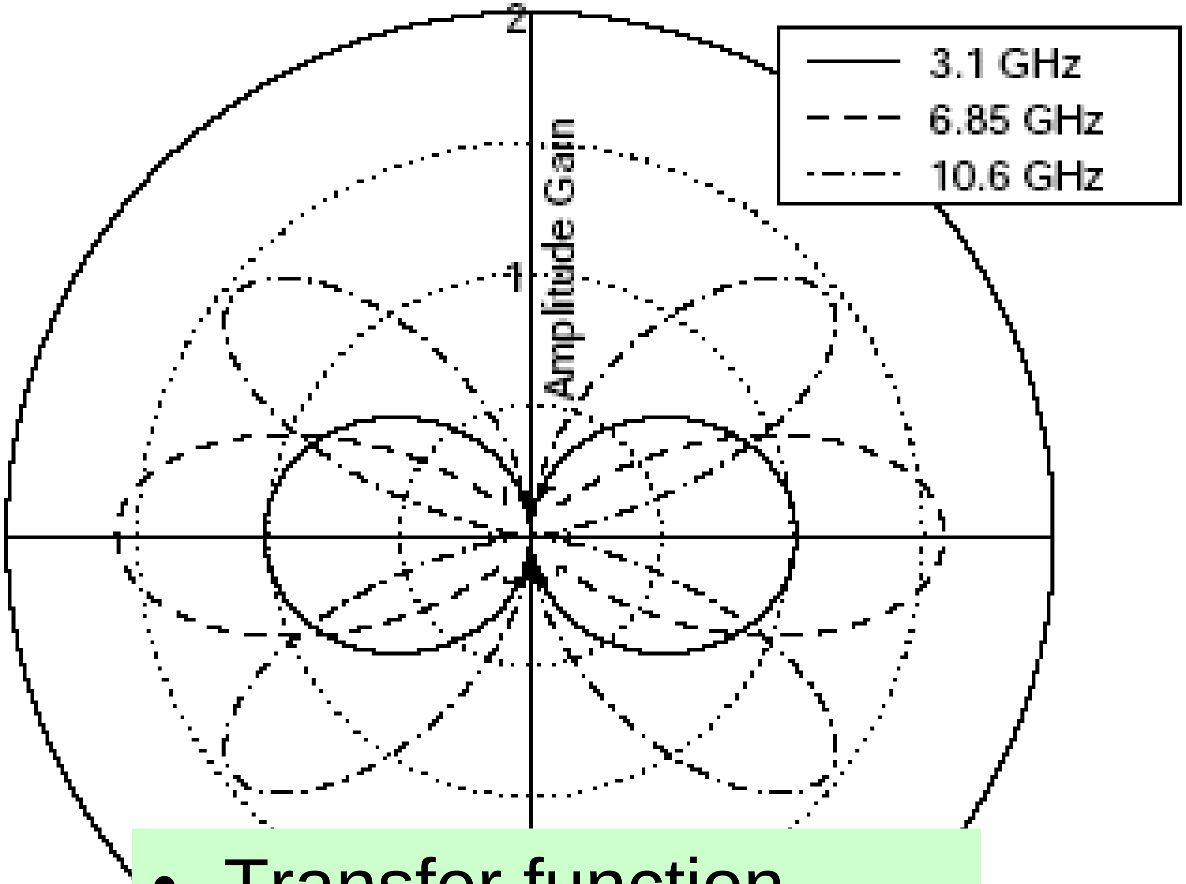

- Transfer function
  - Frequency dependent
  - Angular dependent

Directional Transfer Function of Antenna

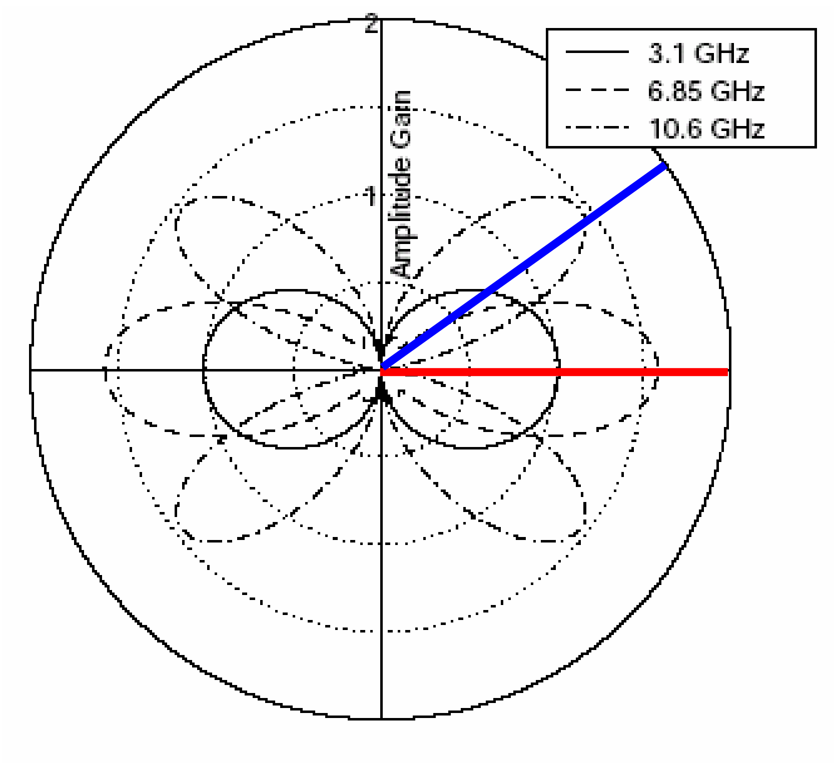

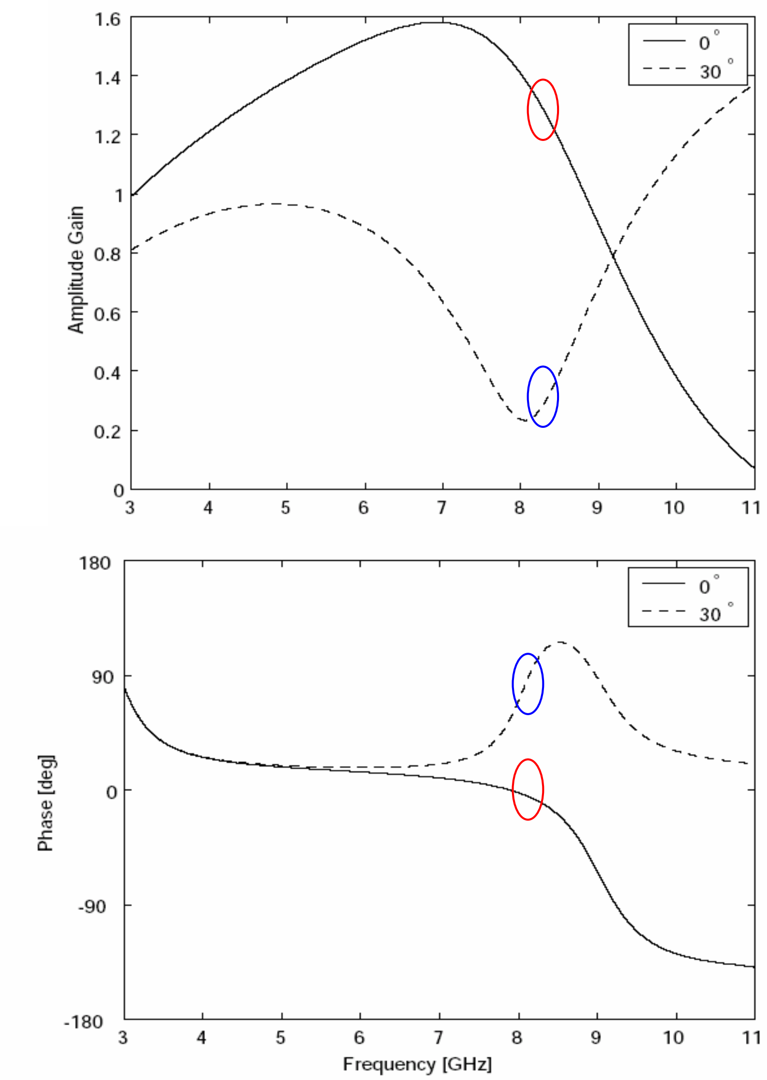

Drastically changed by direction

Directional Impulse Response of Antenna

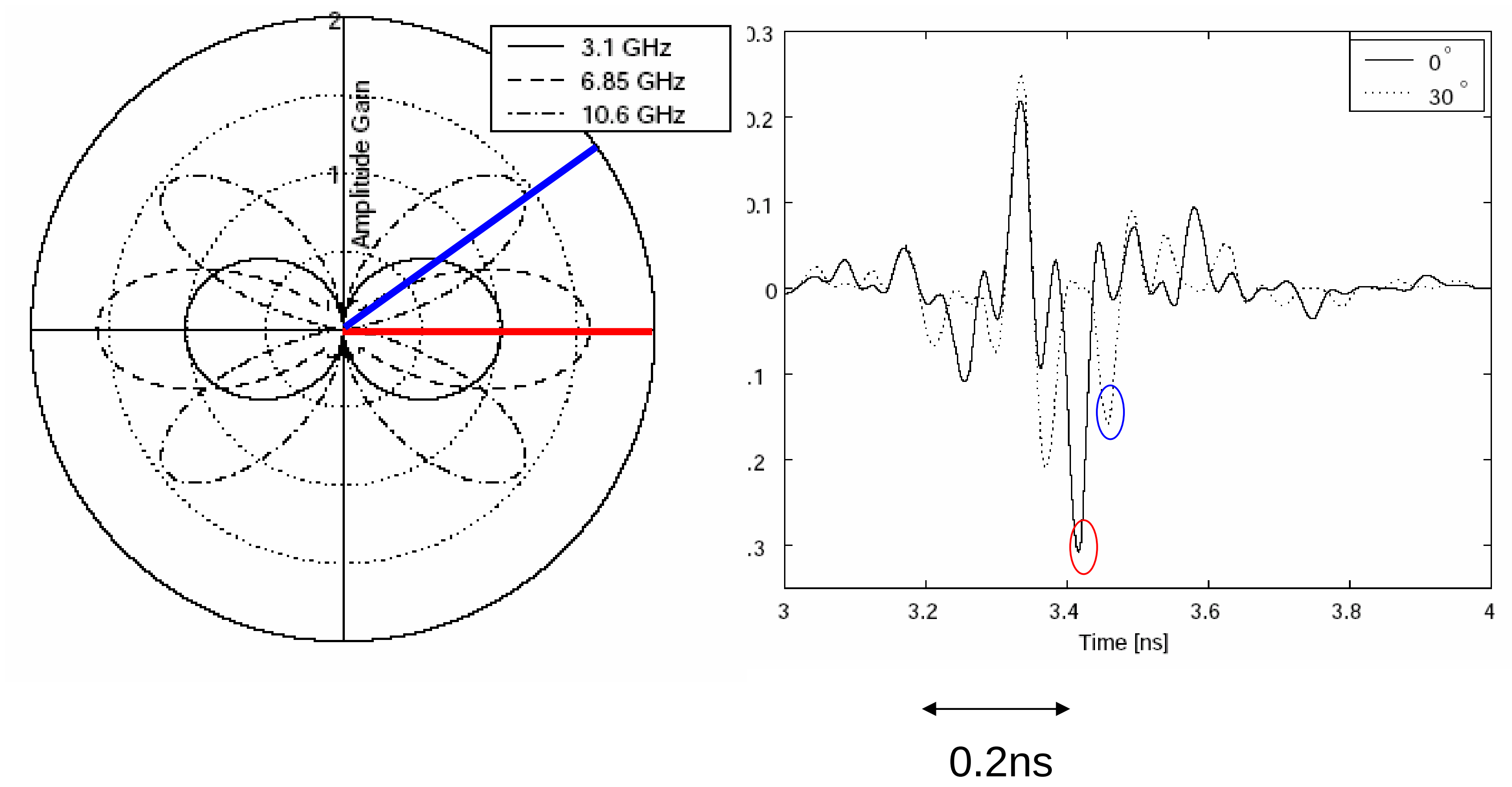

Conventional System vs UWB

Antenna and propagation issues

	Conventional systems	UWB-IR
Antenna	Gain (frequency flat)	Distortion
Multipath	Distortion	Distinction

Conventional Channel Model

IEEE 802.15.3a Model

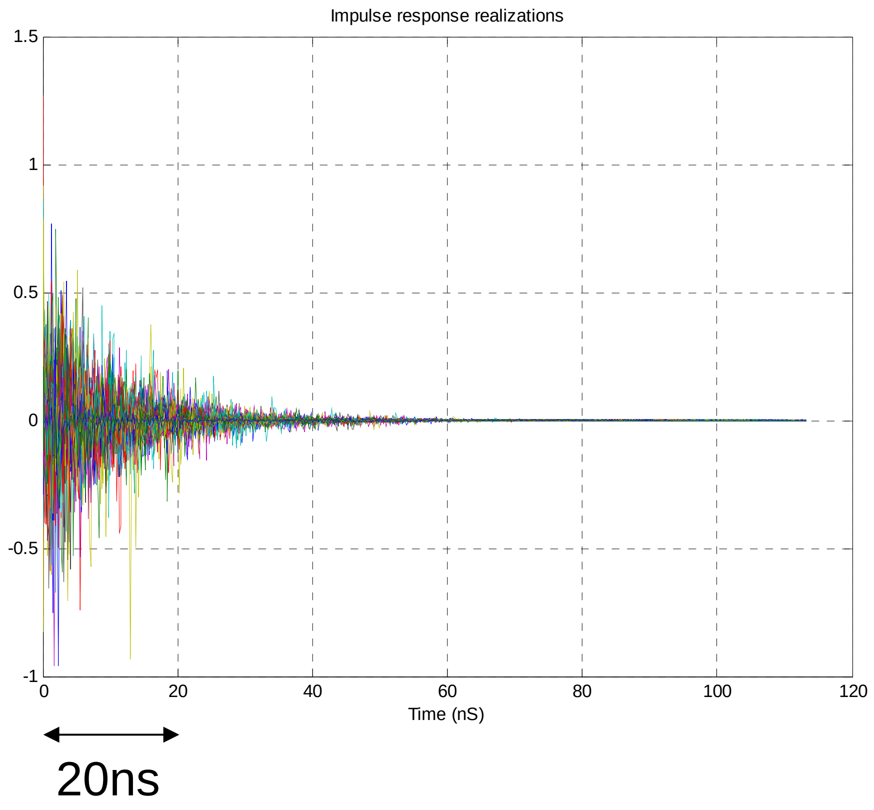

Channel includes antennas and propagation

Valid only for test antennas (omni) !

Channel Modeling Approach of UWB

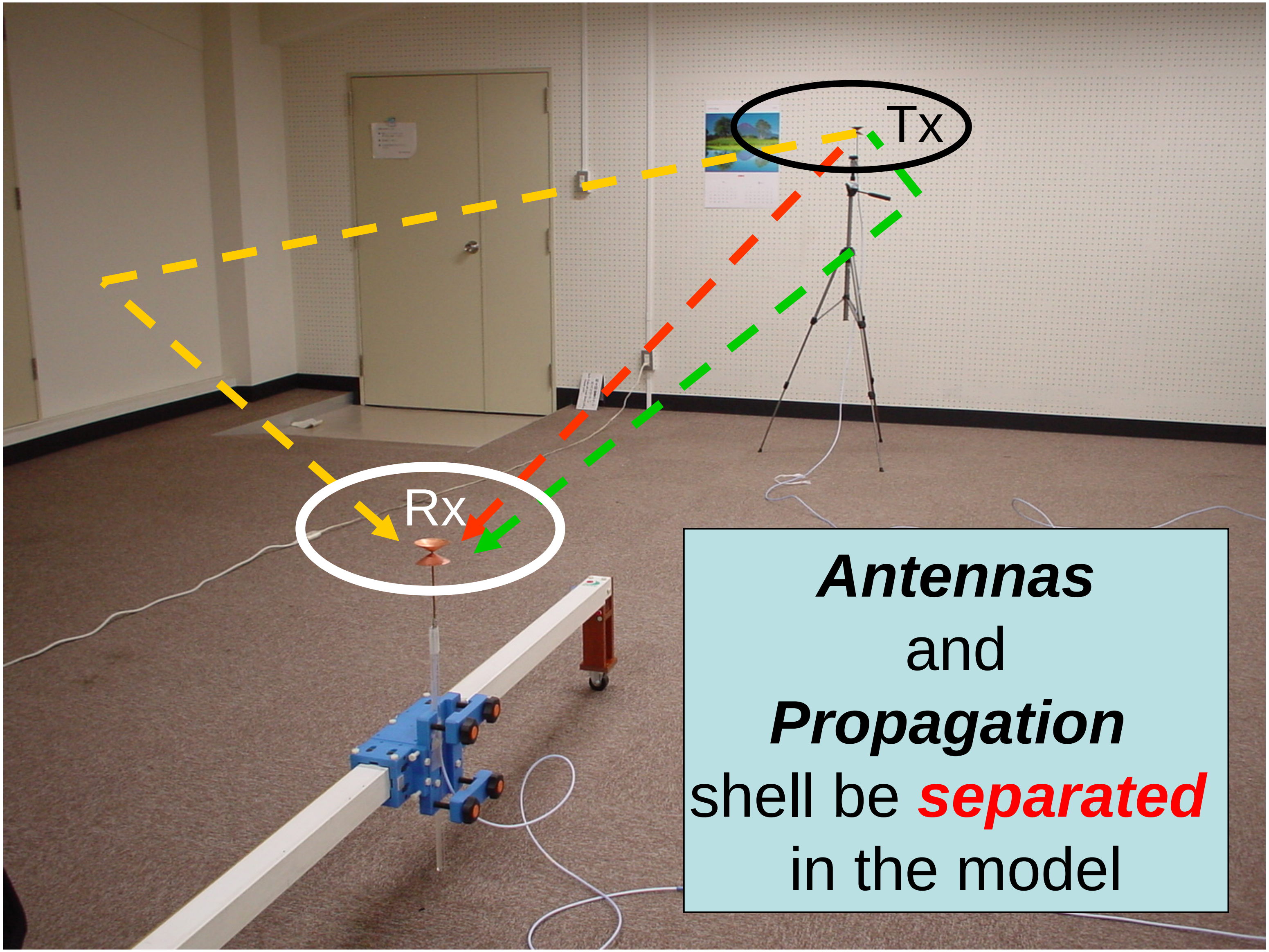

Antenna Model Parameters

Directive Polarimetric Frequency Transfer Function

$$\mathbf{H}_{\mathrm{Ant}}(f,\theta,\varphi)=\hat{\boldsymbol{\theta}}(\theta,\varphi)H_{\theta,\mathrm{Ant}}(f,\theta,\varphi)+\hat{\varphi}(\theta,\varphi)H_{\varphi,\mathrm{Ant}}(f,\theta,\varphi)$$

Solid angle

$$\boldsymbol{\Omega}=(\theta,\varphi)$$

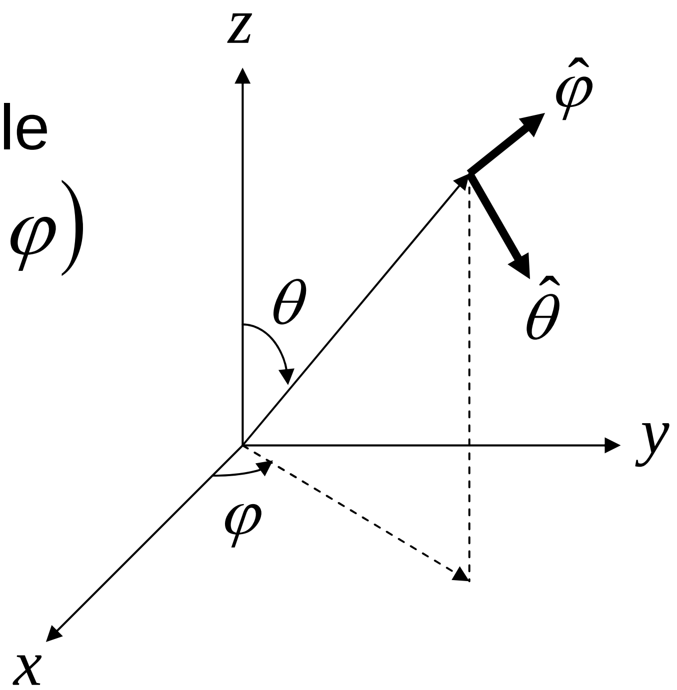

How to Get Antenna Model Parameters

- Electromagnetic (EM) wave simulator
  - MoM (NEC, FEKO, …)
  - FEM (HFSS, …)
  - FDTD (XFDTD, …)
  - …
- Spherical polarimetric measurement
  - Three antenna method for testing antenna calibration

Propagation Modeling

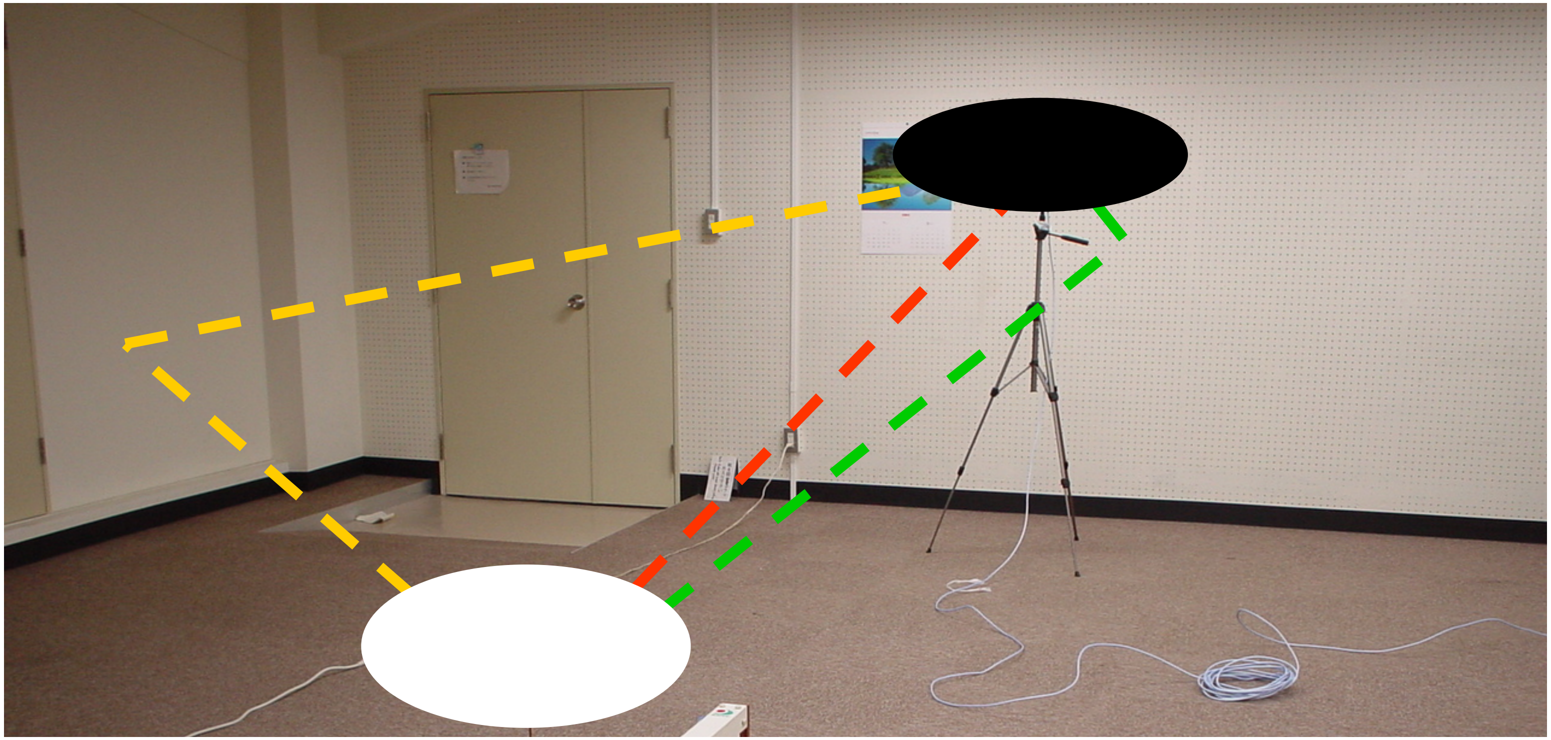

Double-directional model

- Direction of departure (DoD)
- Direction of arrival (DoA)
- Delay time (DT)
- Magnitude (polarimetric, frequency dependent)

Double Directional Ray Model

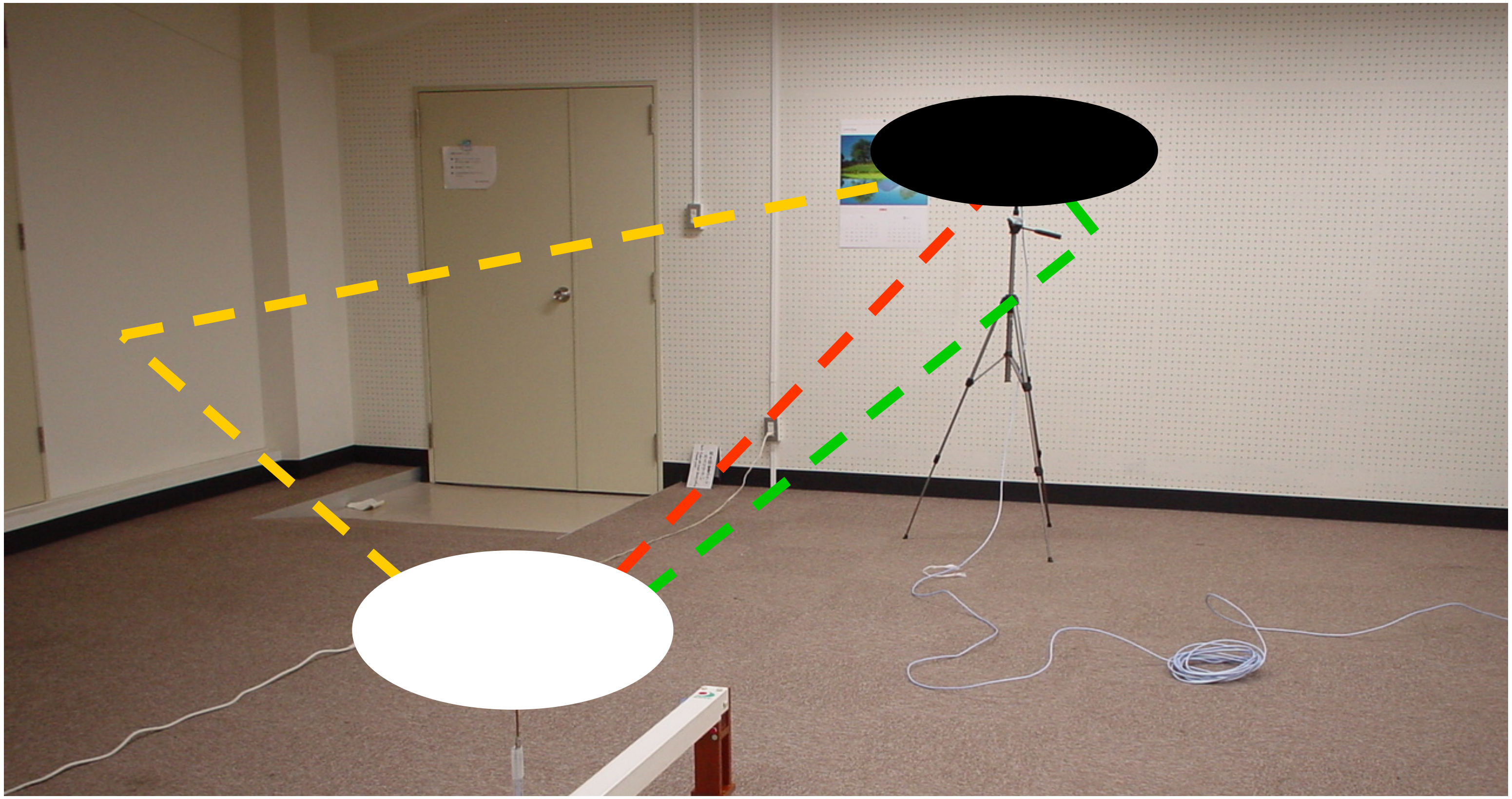

$$H_{\mathrm{Multipath}}\left(f,\mathbf{\Omega}_{\mathrm{Tx}},\mathbf{\Omega}_{\mathrm{Rx}}\right)=$$

$$\sum_{l=1}^{L} a_l(f)\,\delta\left(\mathbf{\Omega}_{\mathrm{Tx}}-\mathbf{\Omega}_{\mathrm{Tx},l}\right)\delta\left(\mathbf{\Omega}_{\mathrm{Rx}}-\mathbf{\Omega}_{\mathrm{Rx},l}\right)\exp\left(-\mathrm{j}2\pi f\tau_l\right)$$

Double Directional Channel Model

… has been studied for MIMO systems

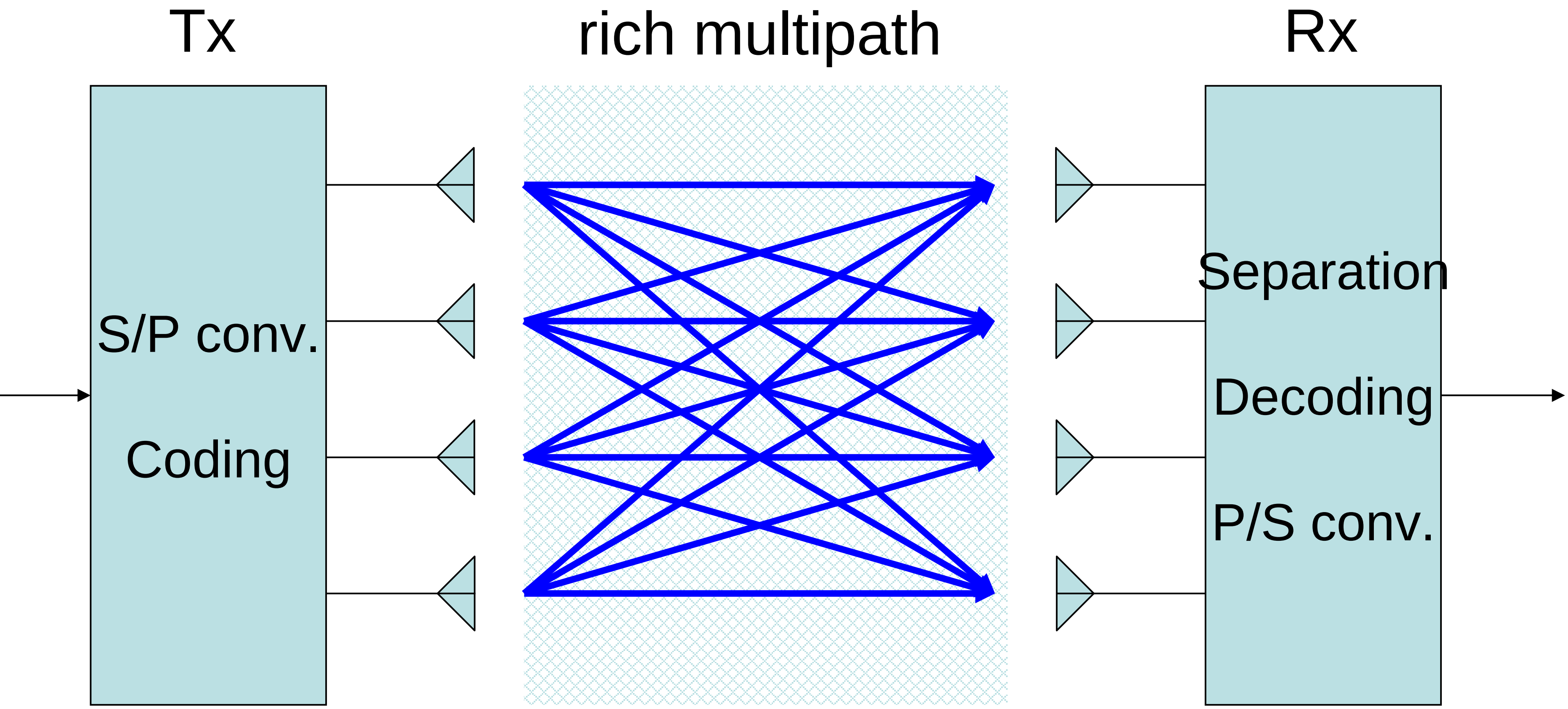

MIMO Antennas

Design of array antenna is a key issue of MIMO channel capacity.

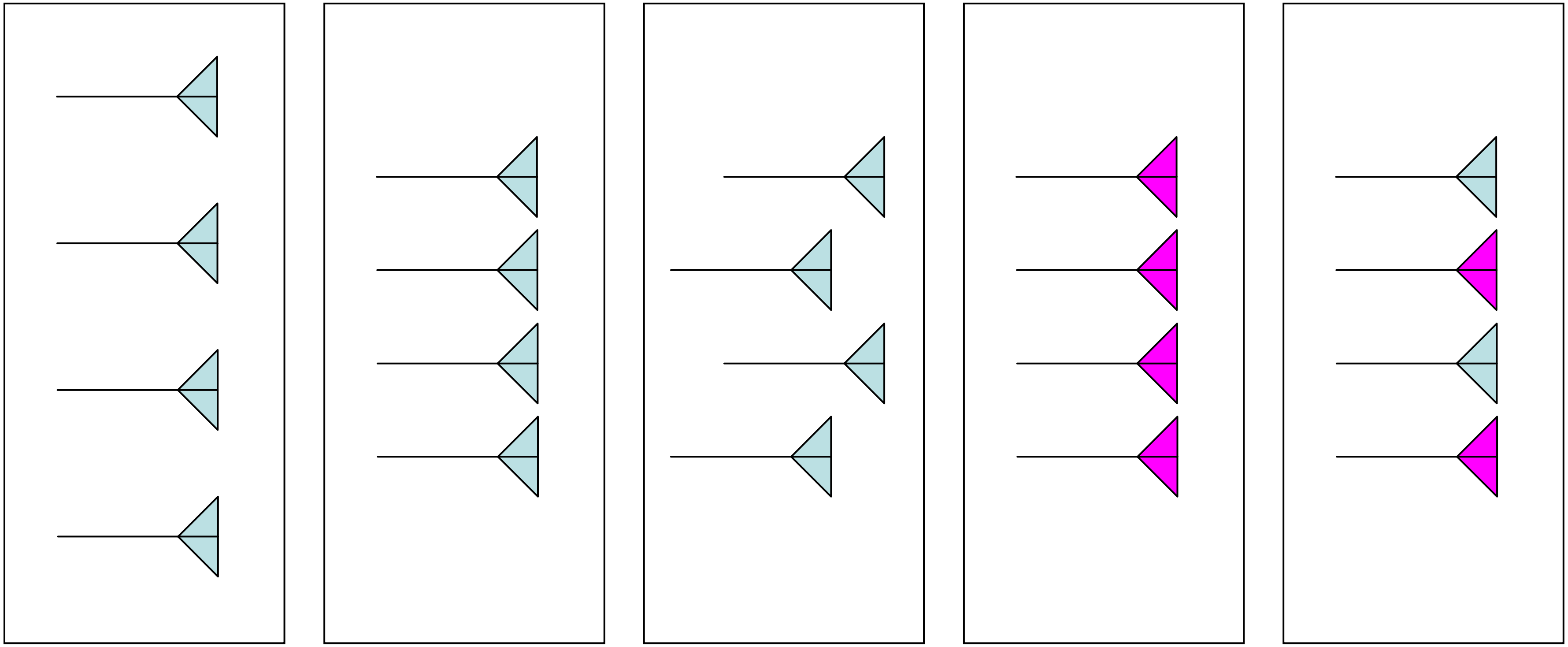

MIMO Channel Matrix

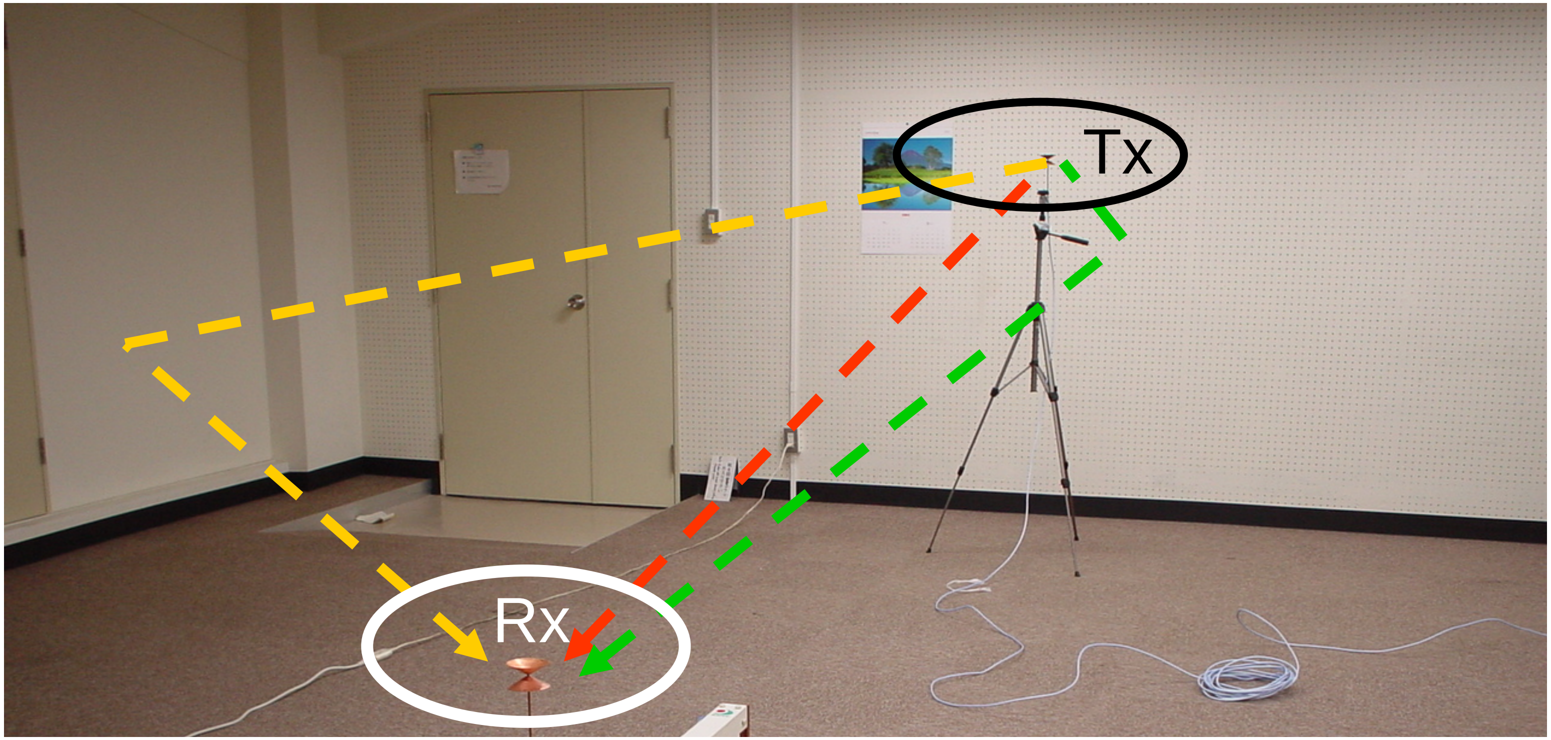

$$\overline{\overline{H}}(f) = \oiint_{\text{Tx}} \oiint_{\text{Rx}} \overline{H}_{\text{Rx}}(f, \mathbf{\Omega}_{\text{Rx}}) H_{\text{Multipath}}(f, \mathbf{\Omega}_{\text{Tx}}, \mathbf{\Omega}_{\text{Rx}}) \overline{H}_{\text{Tx}}^{\text{H}}(f, \mathbf{\Omega}_{\text{Tx}}) \, \mathrm{d}\mathbf{\Omega}_{\text{Rx}} \, \mathrm{d}\mathbf{\Omega}_{\text{Tx}}$$

Rx antenna array vector

Tx antenna array vector

MIMO vs UWB

Antenna and propagation issues

	MIMO	UWB-IR
Antenna	Array configuration	Frequency distortion
Multipath	Double directional	
Magnitude	Frequency flat	Frequency dispersive

Propagation modeling approaches are the same.

Two different aspects of propagation model

- Transmission system design
  - Stochastic, site generic
- Equipment design and installation
  - More deterministic, site specific

UWB Channel Sounding

Time domain vs Frequency domain

	Time domain (Pulse)	Frequency domain (VNA)
Tx Power	Large	Small
Calibration	Difficult	Easy
Data processing	• Raw data • Deconvolution	• Fourier transform • Superresolution (subspace/ML)
Resolution	Fourier	High resolution

UWB Channel Sounding

Directive antenna vs Array antenna

	 Directive antenna	 Array antenna
Tx Power	Small	Large
Sync.	Timing	Timing and phase
Data processing	• Raw data • Deconvolution	• Fourier transform • Superresolution (subspace/ML)
Resolution	Fourier	High resolution

UWB Channel Sounding

Real array vs Synthetic array

	Real array 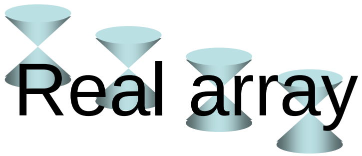	Synthetic array 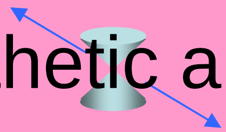
Realization	Multiple antennas RF switch	Scanning
Measurement time	Short	Long
Mutual coupling	To be compensated	None
Antenna spacing	Limited by antenna size	No restriction

UWB Channel Sounding System

- Vector network analyzer + antenna positioner
  - Measurement of spatial transfer function automatically

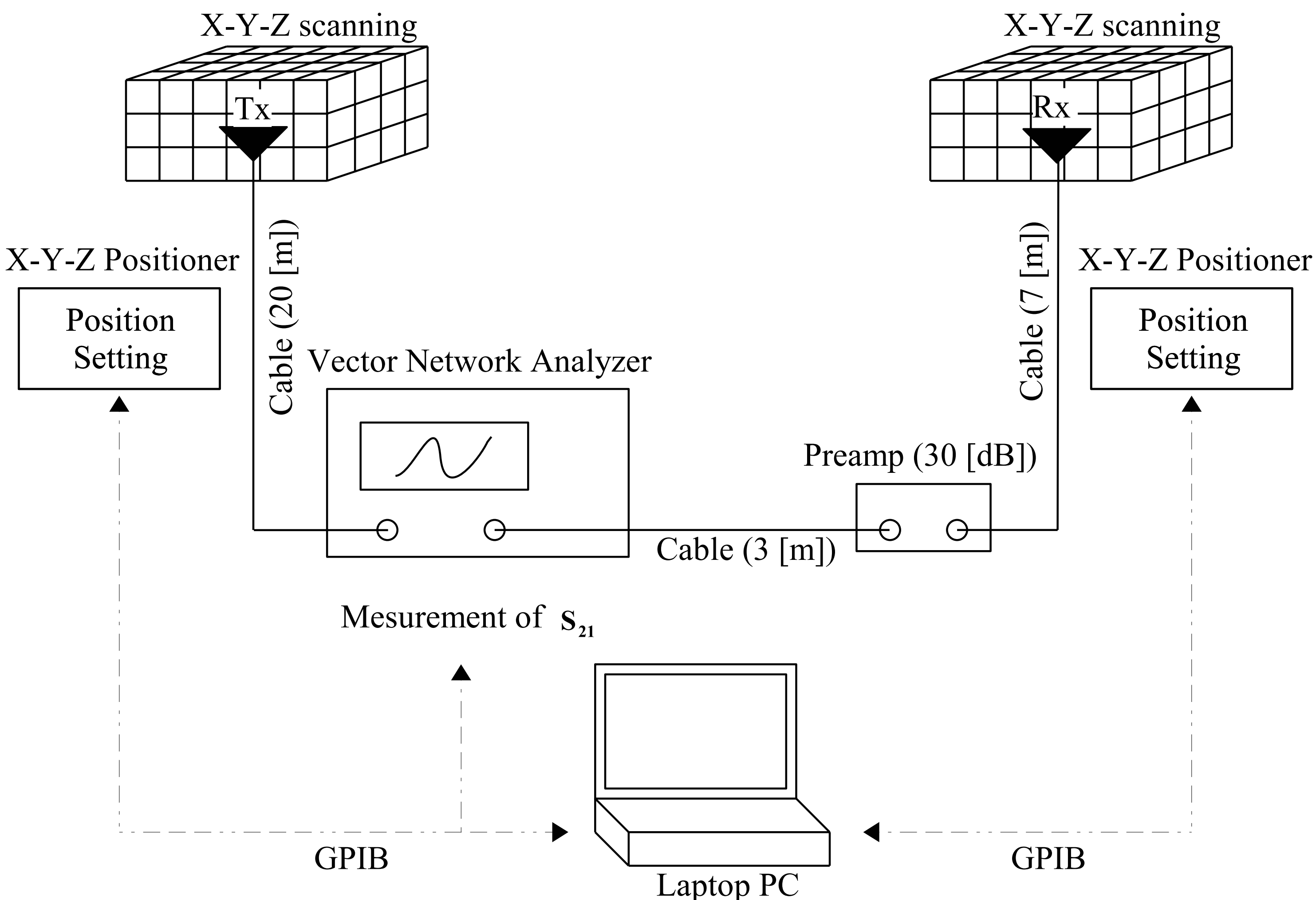

UWB Channel Sounding System

- Architecture
  - Frequency domain → – VNA
  - Synthetic array → – XY positioner

- Pros and Cons
  - Short range ~ low power handling
    - Output power
    - Cable loss
  - Antenna scanning
    - Static environment
    - No array calibration

Double Directional Channel Model

- Discrete path model
  - Channel consists of discrete ray paths

$$h_l(f) = h_0(f,\tau_l) \sum_{\beta_r=\psi,\phi} \sum_{\beta_t=\psi,\phi} \gamma_{\beta_r\beta_t l}(f) D_{r\beta_r}(f,\mathbf{\Omega}_{rl}) D_{t\beta_t}(f,\mathbf{\Omega}_{tl}), \quad (21.3)$$

- $h_l(f)$: Path transfer function
- $h_0(f,\tau_l)$: Free space path loss
- $\sum_{\beta_r=\psi,\phi} \sum_{\beta_t=\psi,\phi}$: Sum with respect to polarizations
- $\gamma_{\beta_r\beta_t l}(f)$: Excess path loss
- $D_{r\beta_r}(f,\mathbf{\Omega}_{rl})$: Rx complex directivity
- $D_{t\beta_t}(f,\mathbf{\Omega}_{tl})$: Tx complex directivity

- Multipath model

$$H(f) = \sum_{l=1}^{L} h_l(f)$$

Model of Synthetic Array

- Complex gain changes due to position

$$D_{\mathrm{r}\beta m_{\mathrm{r}}}(f,\mathbf{\Omega}_{\mathrm{r}}) = D_{\mathrm{r}\beta}(f,\mathbf{\Omega}_{\mathrm{r}})\exp\left(\mathrm{j}\frac{2\pi f}{c}\mathbf{r}_{\mathrm{r}m_{\mathrm{r}}}\cdot\hat{\boldsymbol{\omega}}_{\mathrm{r}}\right). \qquad (21.6)$$

$$\mathbf{r}_{\mathrm{r}m_{\mathrm{r}}} = \hat{\mathbf{x}}x_{\mathrm{r}m_{\mathrm{r}}} + \hat{\mathbf{y}}y_{\mathrm{r}m_{\mathrm{r}}} + \hat{\mathbf{z}}z_{\mathrm{r}m_{\mathrm{r}}}, \qquad (21.5)$$

Position vector

$$\hat{\boldsymbol{\omega}}_{\mathrm{r}} = \hat{\mathbf{x}}\cos\psi_{\mathrm{r}}\cos\phi_{\mathrm{r}} + \hat{\mathbf{y}}\cos\psi_{\mathrm{r}}\sin\phi_{\mathrm{r}} + \hat{\mathbf{z}}\sin\psi_{\mathrm{r}}. \qquad (21.7)$$

Propagation vector

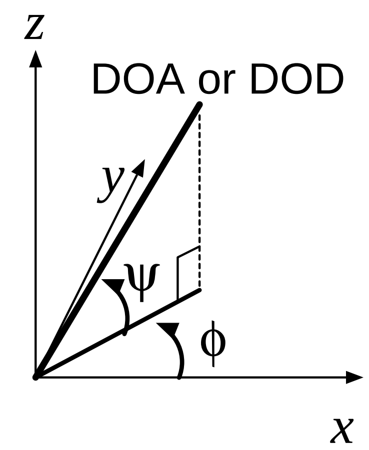

Subband Model

$$h_l(f) = h_0(f, \tau_l) \sum_{\beta_{\mathrm{r}}=\psi,\phi} \sum_{\beta_{\mathrm{t}}=\psi,\phi} \gamma_{\beta_{\mathrm{r}}\beta_{\mathrm{t}}l}(f) D_{\mathrm{r}\beta_{\mathrm{r}}}(f, \mathbf{\Omega}_{\mathrm{r}l}) D_{\mathrm{t}\beta_{\mathrm{t}}}(f, \mathbf{\Omega}_{\mathrm{t}l}), \qquad (21.9)$$

- γ can not be considered as constant over UWB bandwidth.
  - Piecewise constant

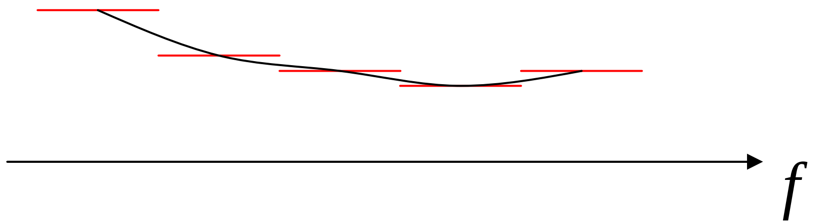

Spherical Wave Model

- For short range paths, plane wave approximation is not appropriate.
  - Spherical wave model

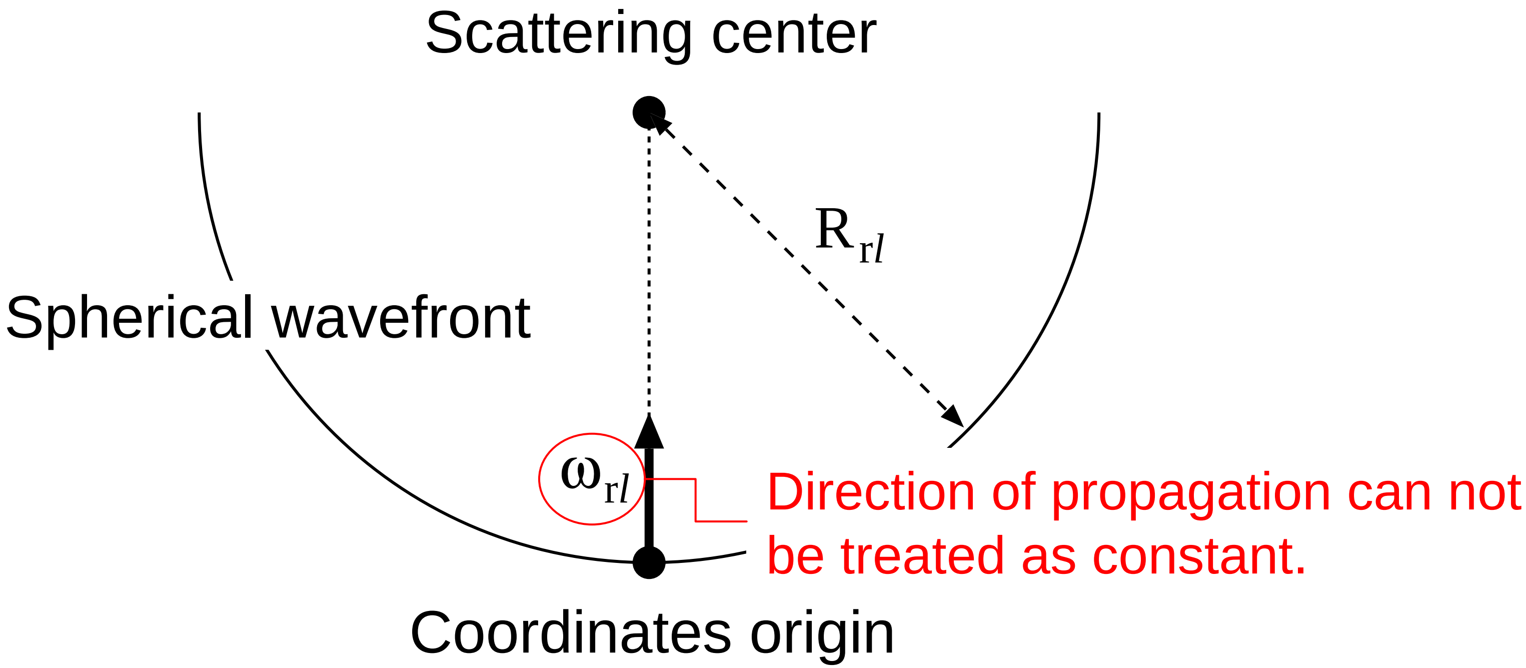

Spherical Wave Model at Rx Array

$$h_{lm_\mathrm{t}m_\mathrm{r}}(f) = h_0(f,\tau_l)\gamma_l(f)D_\mathrm{r}(f,\mathbf{\Omega}_{\mathrm{r}l})D_\mathrm{t}(f,\mathbf{\Omega}_{\mathrm{t}l})$$

$$\exp\left[\mathrm{j}\frac{2\pi f}{c}\left(\left\|\mathbf{R}_{\mathrm{r}l}-\mathbf{r}_{\mathrm{r}m_\mathrm{r}}\right\|-R_{\mathrm{r}l}\right)\right]\exp\left(-\mathrm{j}\frac{2\pi f}{c}\mathbf{r}_{\mathrm{t}m_\mathrm{t}}\cdot\hat{\boldsymbol{\omega}}_{\mathrm{t}l}\right). \quad (21.9)$$

Phase delay correction wrt origin

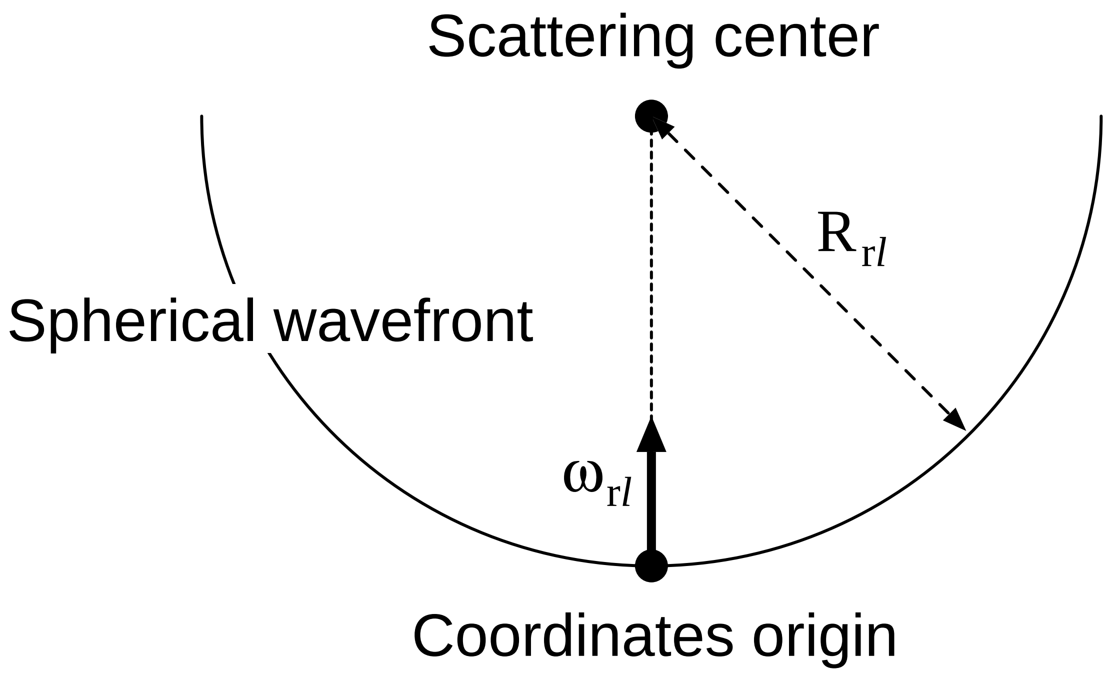

Issue on Spherical Wave Model

- Not always compatible with double-directional model

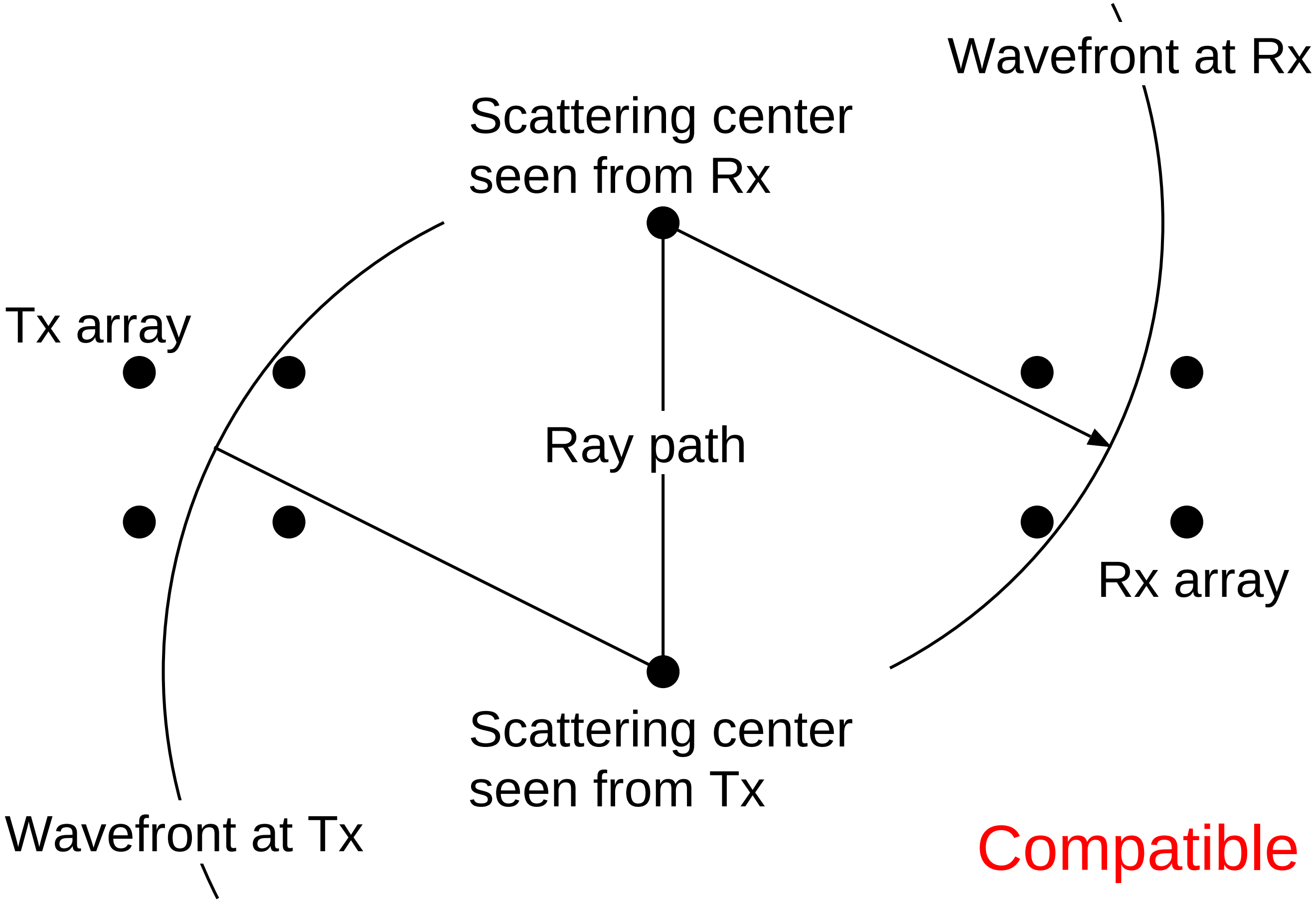

Compatible case

Issue on Spherical Wave Model

- Not always compatible with double-directional model

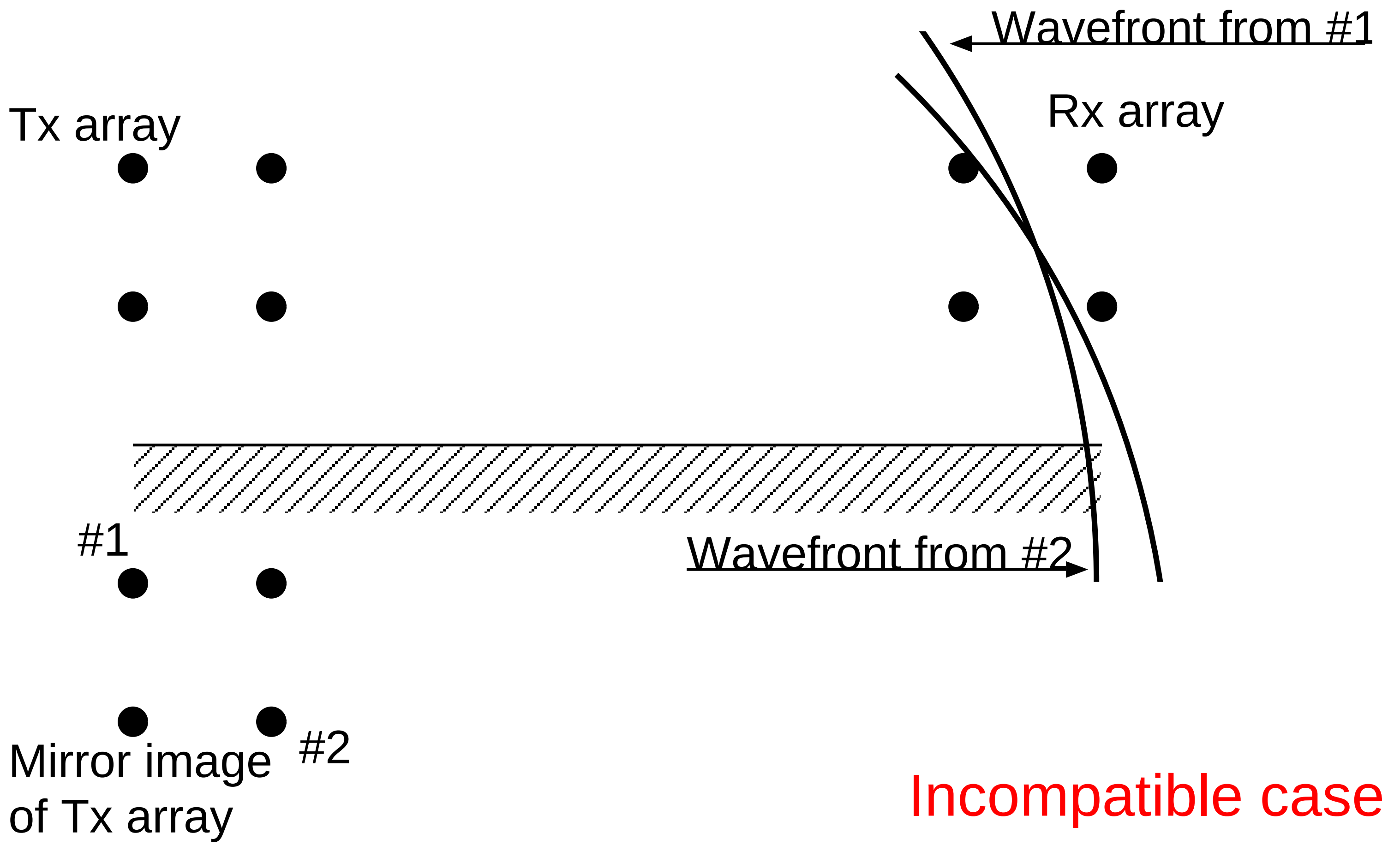

Issue on Spherical Wave Model

- SIMO and MISO (single-directional) processing
- Matching by using ray-tracing
  - Accurate time delay due to UWB

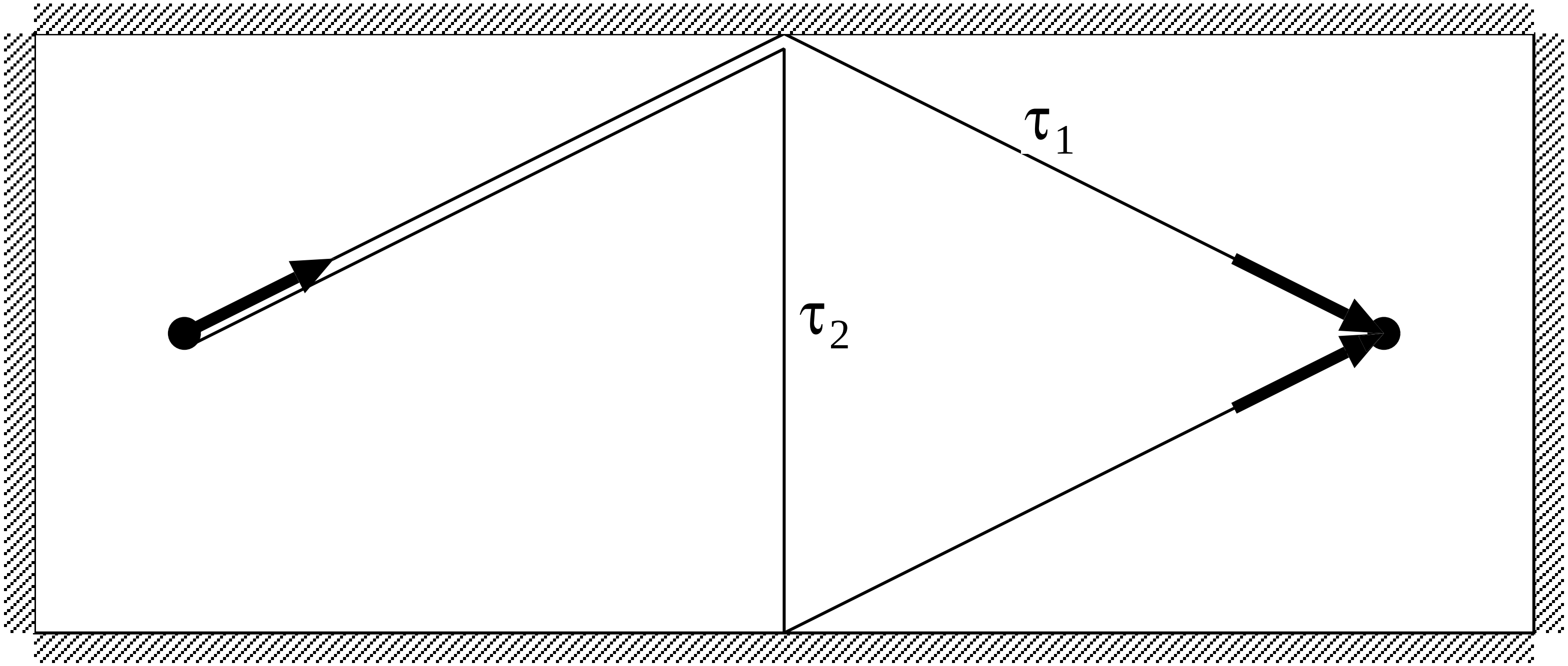

Channel Parameter Estimation

- Parametric channel model
  - Free from antenna geometry
  - Resolution still influenced by measurement configuration

$$h_{lm_{\mathrm{t}}m_{\mathrm{r}}}(f) = h_0(f,\tau_l)\gamma_l(f)D_{\mathrm{r}}(f,\mathbf{\Omega}_{\mathrm{r}l})D_{\mathrm{t}}(f,\mathbf{\Omega}_{\mathrm{t}l}) \exp\left[\mathrm{j}\frac{2\pi f}{c}\left(\left\|\mathbf{R}_{\mathrm{r}l}-\mathbf{r}_{\mathrm{r}m_{\mathrm{r}}}\right\|-R_{\mathrm{r}l}\right)\right]\exp\left(-\mathrm{j}\frac{2\pi f}{c}\mathbf{r}_{\mathrm{t}m_{\mathrm{t}}}\cdot\hat{\boldsymbol{\omega}}_{\mathrm{t}l}\right). \quad (21.9)$$

Parameters to be estimated

- Two major approaches
  - Subspace based
  - ML based

Parametric Channel Model

- Measured data contaminated by Gaussian noise

$$y_{m_r k} = H_{m_r k} + n_{m_r k}, \qquad (21.11)$$

$$\mathrm{var}(n_{m_r k}) = \sigma^2$$

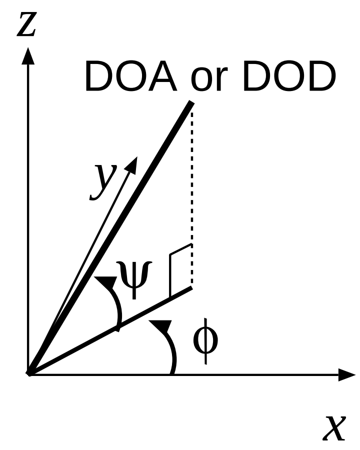

- Parameters to be estimated

$$\boldsymbol{\mu}_l = \left\{ \left\{ \gamma_{li} \right\}_{i=1}^{I}, \psi_{rl}, \phi_{rl}, R_l, \tau_l \right\}, \qquad (21.12)$$

$$\boldsymbol{\mu} = \bigcup_{l=1}^{L} \boldsymbol{\mu}_l. \qquad (21.13)$$

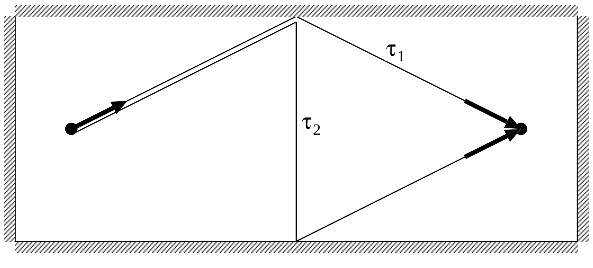

Likelihood Function

- Conditional probability of the observation data assuming parameter set
  - Likelihood function

$$p(\mathbf{y}\,|\,\boldsymbol{\mu}) = \prod_{k=1}^{K} \prod_{m_\mathrm{r}=1}^{M_\mathrm{r}} \left[\frac{1}{\pi\sigma} \exp\left(-\frac{|\, y_{m_\mathrm{r}k} - H_{m_\mathrm{r}k}(\boldsymbol{\mu})\,|^2}{\sigma^2} \right) \right]. \quad (21.15)$$

  - Observed data

$$\mathbf{y} = \{ y_{m_\mathrm{r}k} \,|\, 1 \le m_\mathrm{r} \le M_\mathrm{r}, 1 \le k \le K \} \quad (21.14)$$

- ML estimate
  - $\boldsymbol{\mu}$ maximizing p for given $\mathbf{y}$

Maximum Likelihood Estimation

- Exhaustive joint search of $\boldsymbol{\mu}$

$$p(\mathbf{y} \mid \boldsymbol{\mu}) = \prod_{k=1}^{K} \prod_{m_\mathrm{r}=1}^{M_\mathrm{r}} \left[\frac{1}{\pi\sigma} \exp\left(-\frac{| y_{m_\mathrm{r}k} - H_{m_\mathrm{r}k}(\boldsymbol{\mu}) |^2}{\sigma^2} \right) \right]. \qquad (21.15)$$

Expectation Maximization (EM) Algorithm

- Estimate of "complete data" $\mathbf{x}$ from "incomplete data" $\mathbf{y}$ (E-step)

$$\mathbf{x}_l = \mathbf{h}_l + b_l(\mathbf{y} - \mathbf{H}). \qquad (21.17)$$

- ML applied to "complete data" (M-step)

$$\arg\max_{\boldsymbol{\mu}} p(\mathbf{x}_l \mid \boldsymbol{\mu}) = \boxed{\arg\min_{\boldsymbol{\mu}_l} \left\| \mathbf{x}_l - \mathbf{h}_l(\boldsymbol{\mu}_l) \right\|^2 .} \qquad (21.19)$$

Least square problem

→ to be solved by matched filtering

EM Algorithm and Matched Filtering

- Matched filter detection

$$\boldsymbol{\mu}_l = \arg\max_{\boldsymbol{\mu}_l} \frac{|\mathbf{a}^H(\boldsymbol{\mu}_l)\mathbf{x}_l|}{\sqrt{\mathbf{a}^H(\boldsymbol{\mu}_l)\mathbf{a}(\boldsymbol{\mu}_l)}}. \quad (21.22)$$

$$\hat{\gamma}_{li} = \frac{\mathbf{a}_i^H(\boldsymbol{\mu}_l)\mathbf{x}_{li}}{\mathbf{a}_i^H(\boldsymbol{\mu}_l)\mathbf{a}_i(\boldsymbol{\mu}_l)}, \quad (21.23)$$

Space Alternating EM (SAGE) Algorithm

- Sequential search of parameters

$$\hat{\psi}_{rl} = \arg\max_{\psi_{rl}} \frac{|\mathbf{a}^H(\psi_{rl},\phi_{rl},R_l,\tau_l)\mathbf{x}_l|}{\sqrt{\mathbf{a}^H(\psi_{rl},\phi_{rl},R_l,\tau_l)\mathbf{a}(\psi_{rl},\phi_{rl},R_l,\tau_l)}}, \quad (21.24)$$

$$\hat{\phi}_{rl} = \arg\max_{\phi_{rl}} \frac{|\mathbf{a}^H(\hat{\psi}_{rl},\phi_{rl},R_l,\tau_l)\mathbf{x}_l|}{\sqrt{\mathbf{a}^H(\hat{\psi}_{rl},\phi_{rl},R_l,\tau_l)\mathbf{a}(\hat{\psi}_{rl},\phi_{rl},R_l,\tau_l)}}, \quad (21.25)$$

$$\hat{R}_l = \arg\max_{R_l} \frac{|\mathbf{a}^H(\hat{\psi}_{rl},\hat{\phi}_{rl},R_l,\tau_l)\mathbf{x}_l|}{\sqrt{\mathbf{a}^H(\hat{\psi}_{rl},\hat{\phi}_{rl},R_l,\tau_l)\mathbf{a}(\hat{\psi}_{rl},\hat{\phi}_{rl},R_l,\tau_l)}}, \quad (21.26)$$

$$\hat{\tau}_l = \arg\max_{\tau_l} \frac{|\mathbf{a}^H(\hat{\psi}_{rl},\hat{\phi}_{rl},\hat{R}_l,\tau_l)\mathbf{x}_l|}{\sqrt{\mathbf{a}^H(\hat{\psi}_{rl},\hat{\phi}_{rl},\hat{R}_l,\tau_l)\mathbf{a}(\hat{\psi}_{rl},\hat{\phi}_{rl},\hat{R}_l,\tau_l)}}, \quad (21.27)$$

  – Good initial estimate is necessary.

Successive Cancellation Approach

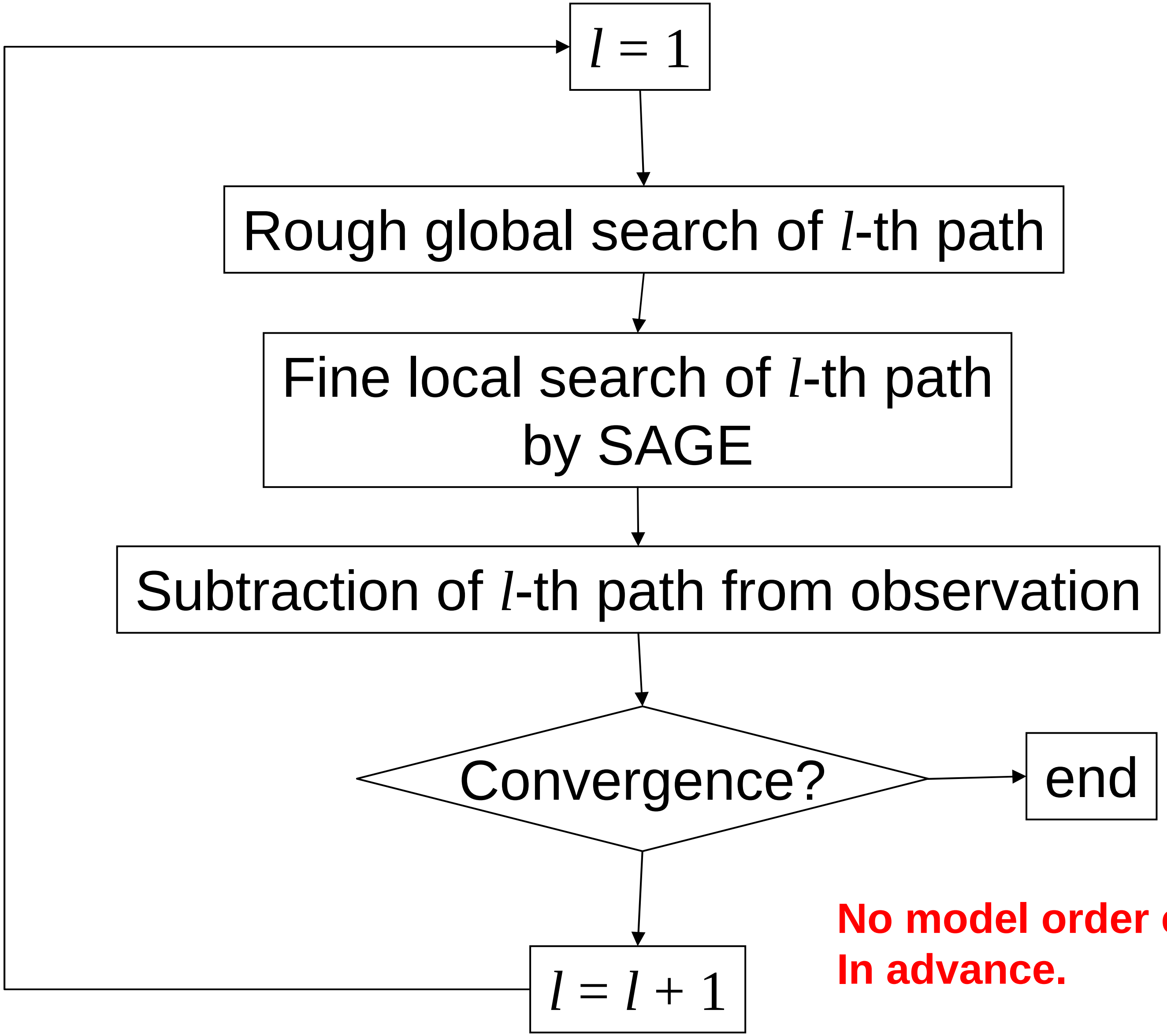

No model order estimation In advance.

Experiment in an Indoor Environment (1)

- Measurement site: an empty room

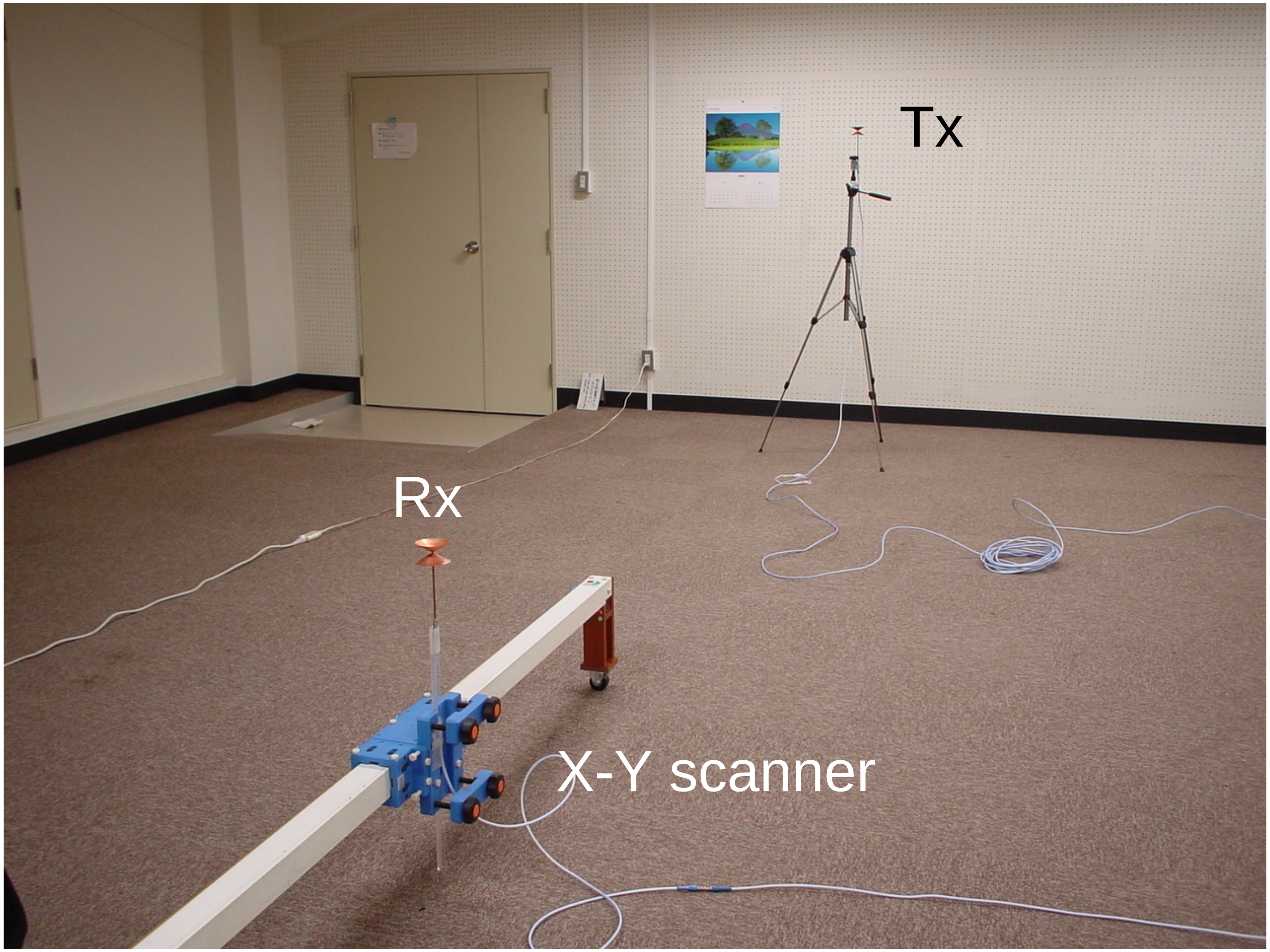

Experiment in an Indoor Environment (2)

- Floor plan of the room

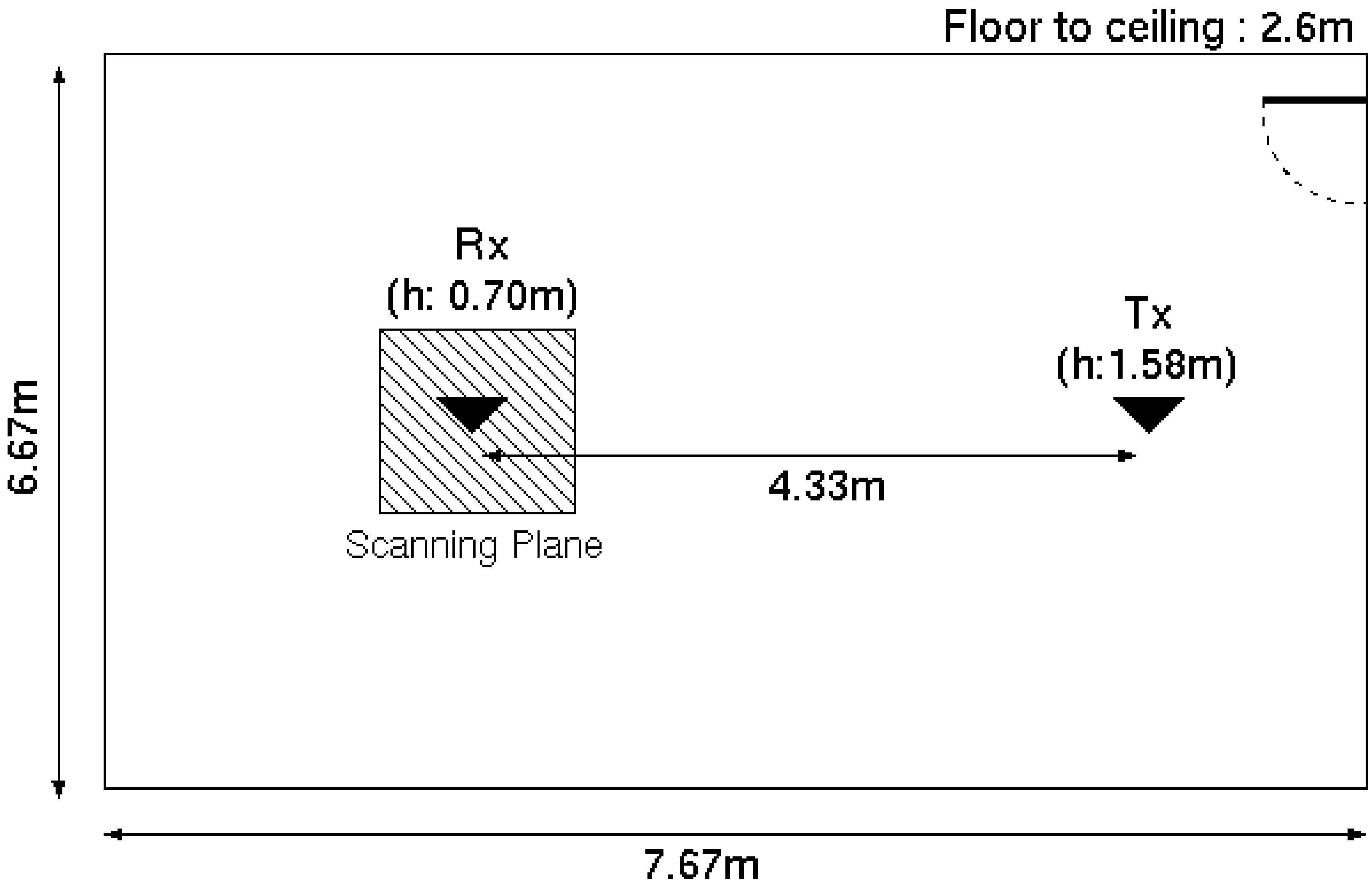

Experiment in an Indoor Environment (3)

- Estimated parameters : DoA (Az, El), DT
- Measured data :
  - Spatially 10 by 10 points at Rx
  - 801 points frequency sweeping from 3.1 to 10.6 [GHz] (sweeping interval: 10 [MHz])
- Antennas : Biconical antennas for Tx and Rx
- Calibration : Function of VNA, back-to-back
- IF Bandwidth of VNA : 100 [Hz]
- Wave polarization : Vertical - Vertical
- Bandwidth of each subband : 800 [MHz]

Measurement Result (1)

- The result of ray path identification

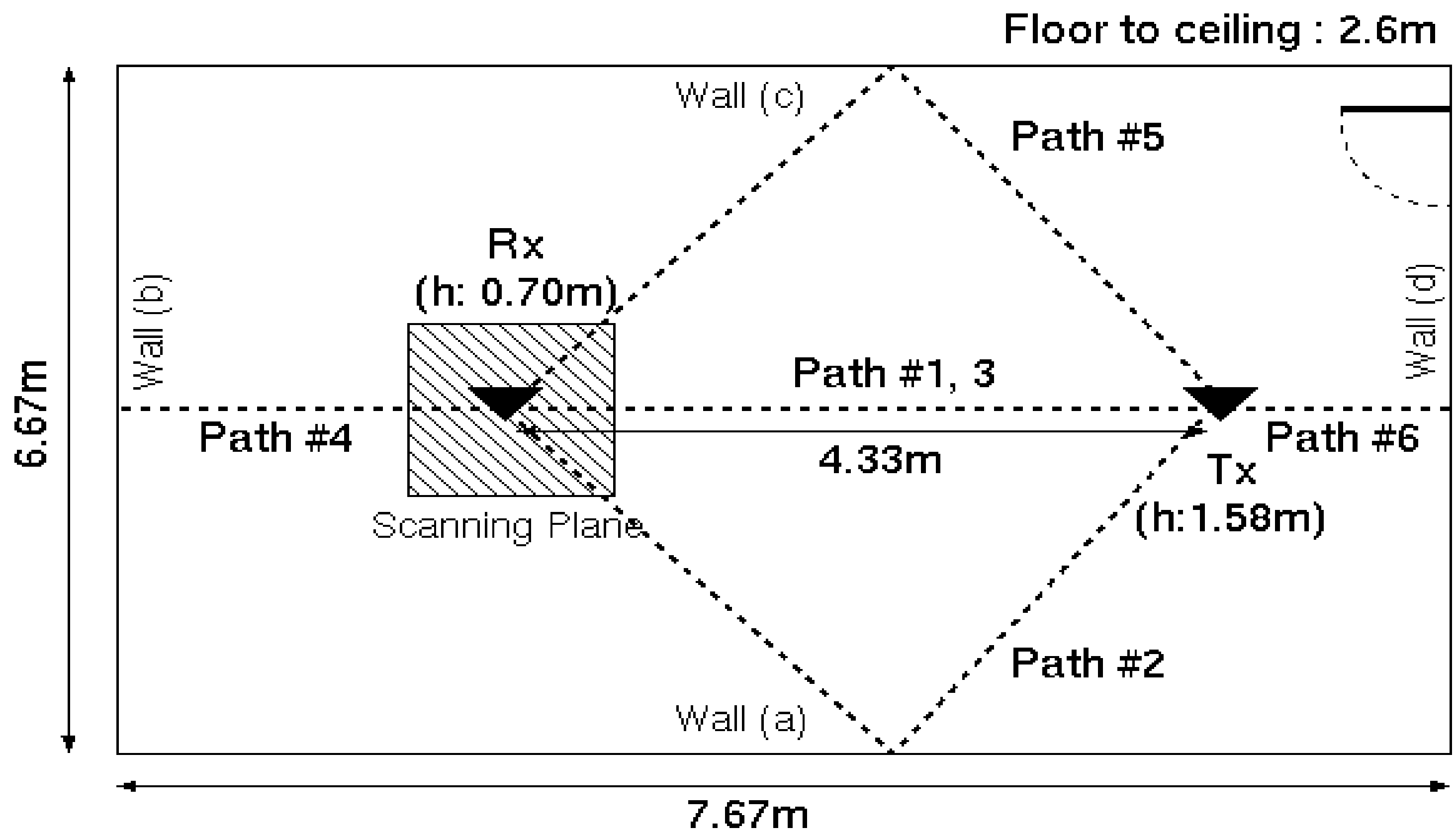

There 6 waves detected and are almost specular waves.

Measurement Result (2)

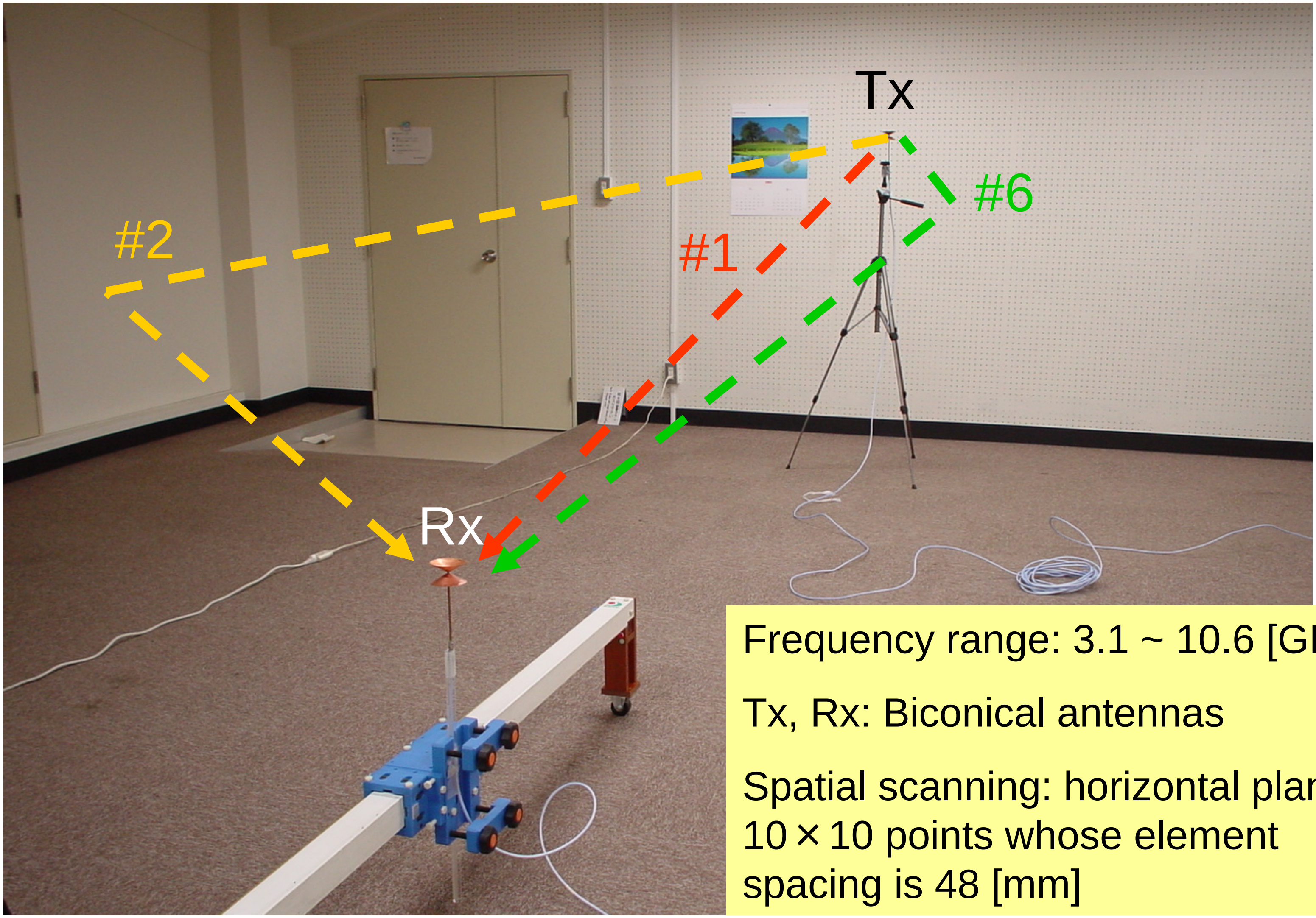

Frequency range: 3.1 ~ 10.6 [GHz]

Tx, Rx: Biconical antennas

Spatial scanning: horizontal plane, 10 × 10 points whose element spacing is 48 [mm]

6 specular waves were observed.

Measurement Result (3)

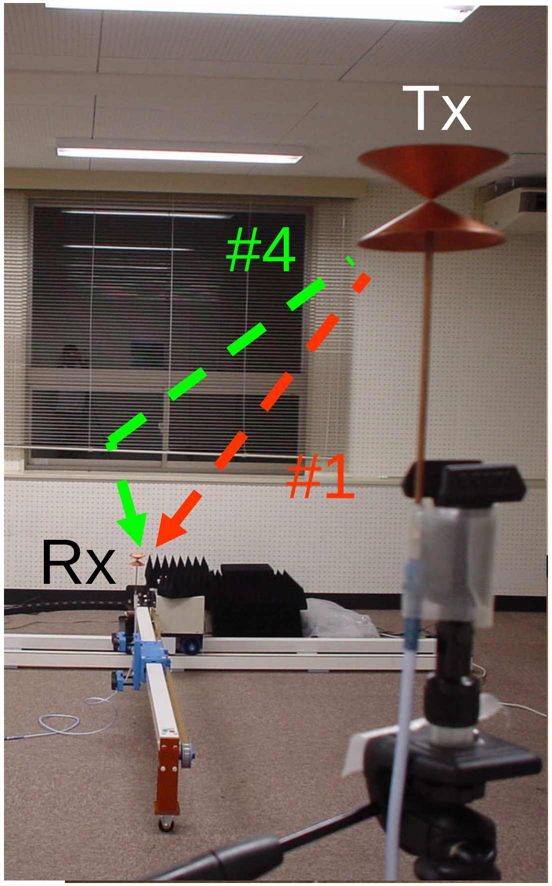

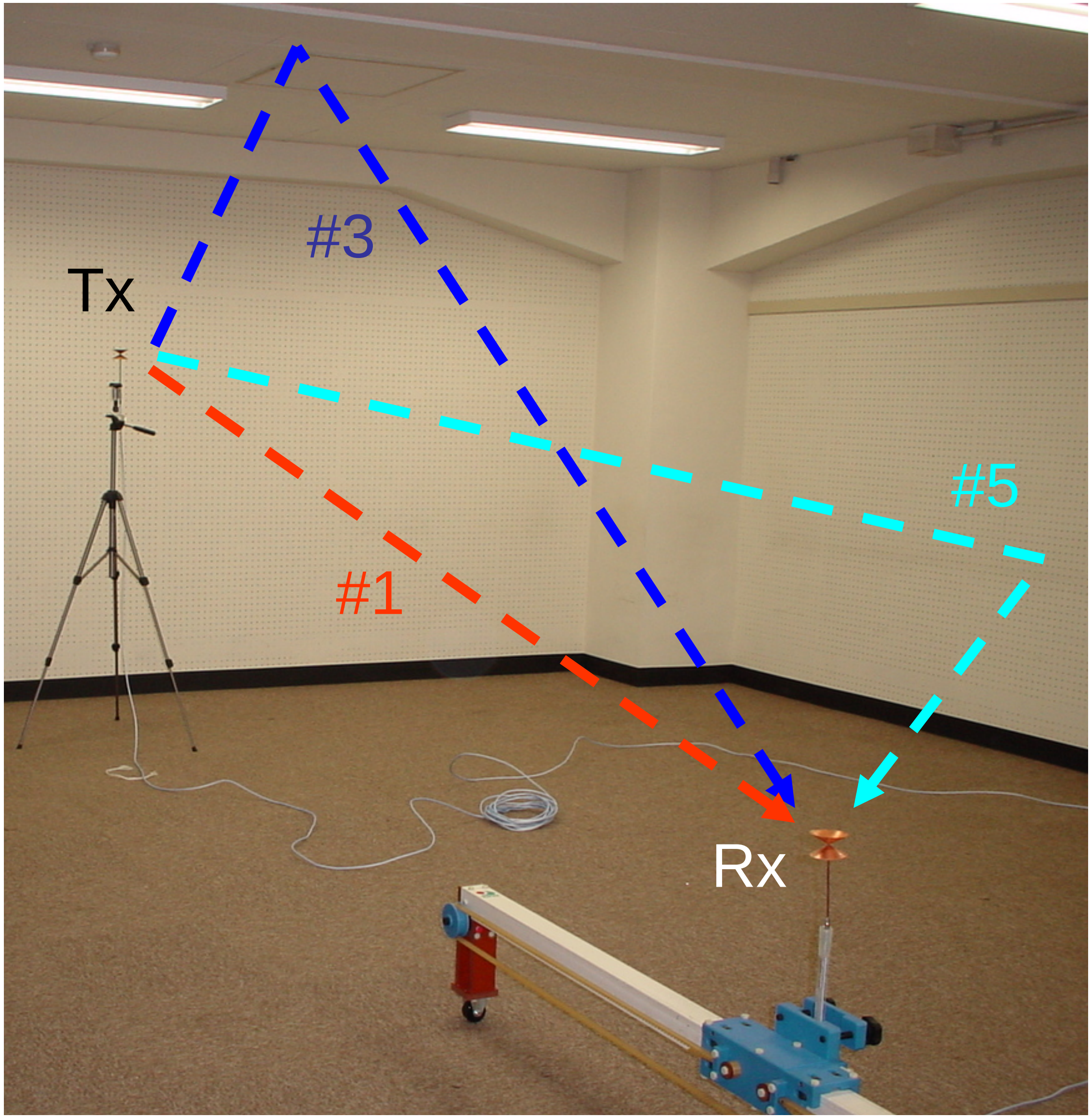

#4 is a reflection from the back of Rx

Measurement Result (4)

- Extracted spectrum of direct wave

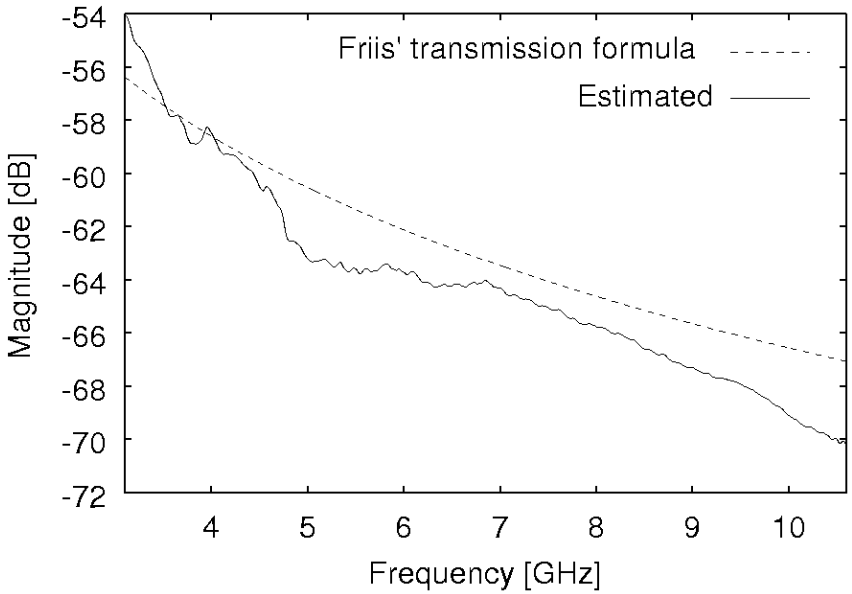

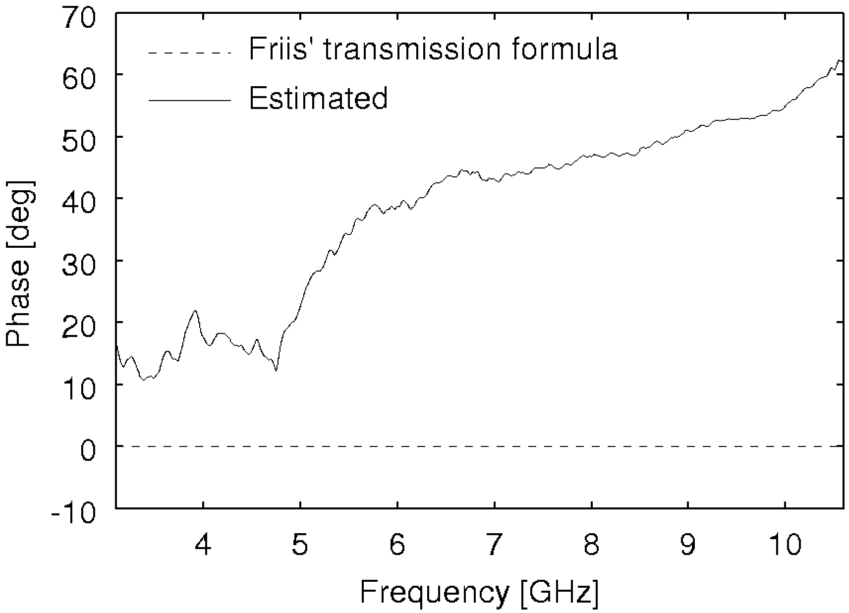

  - Transfer functions of antennas are already deconvolved.
  - The phase component is the deviation from free space phase rotation (ideally flat).

Experiment in an Indoor Environment (4)

- Comparison of the measurement result in 9 different Rx position

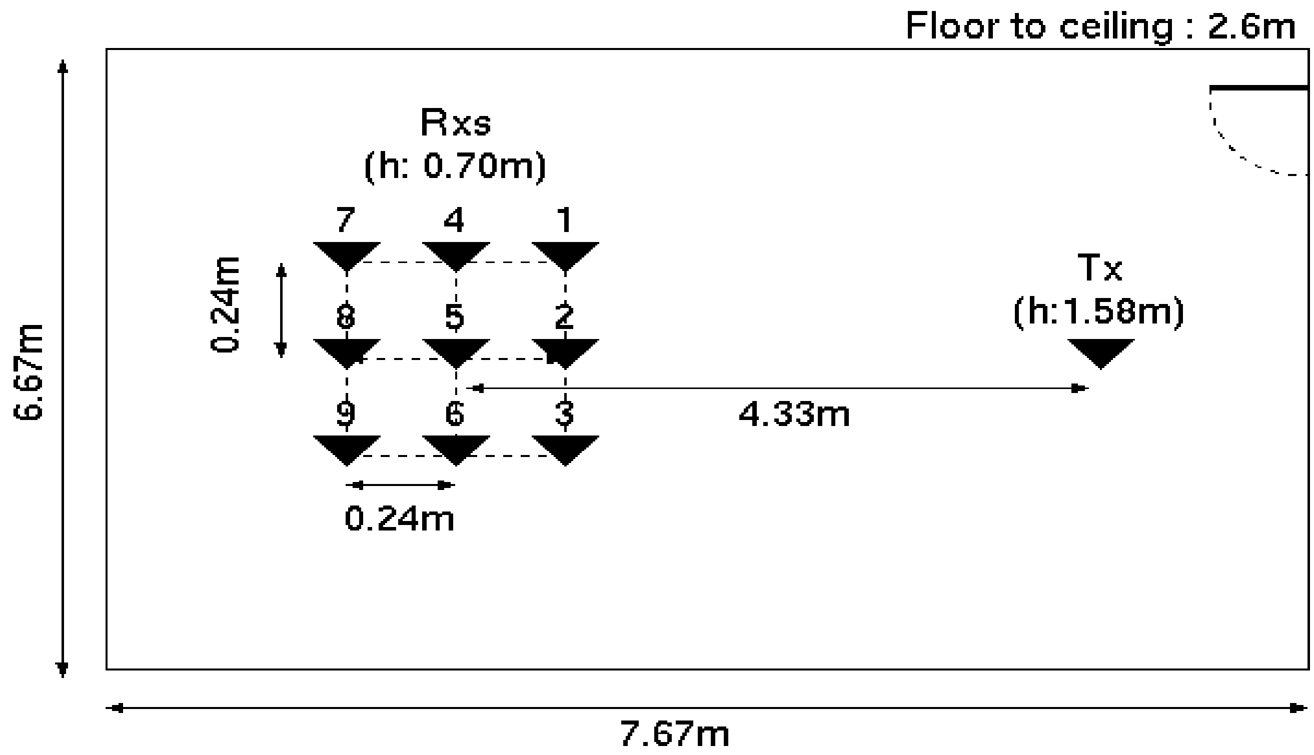

The path type detected in each measurement was almost same.

Measurement Result (5)

- Estimated source position for direct wave

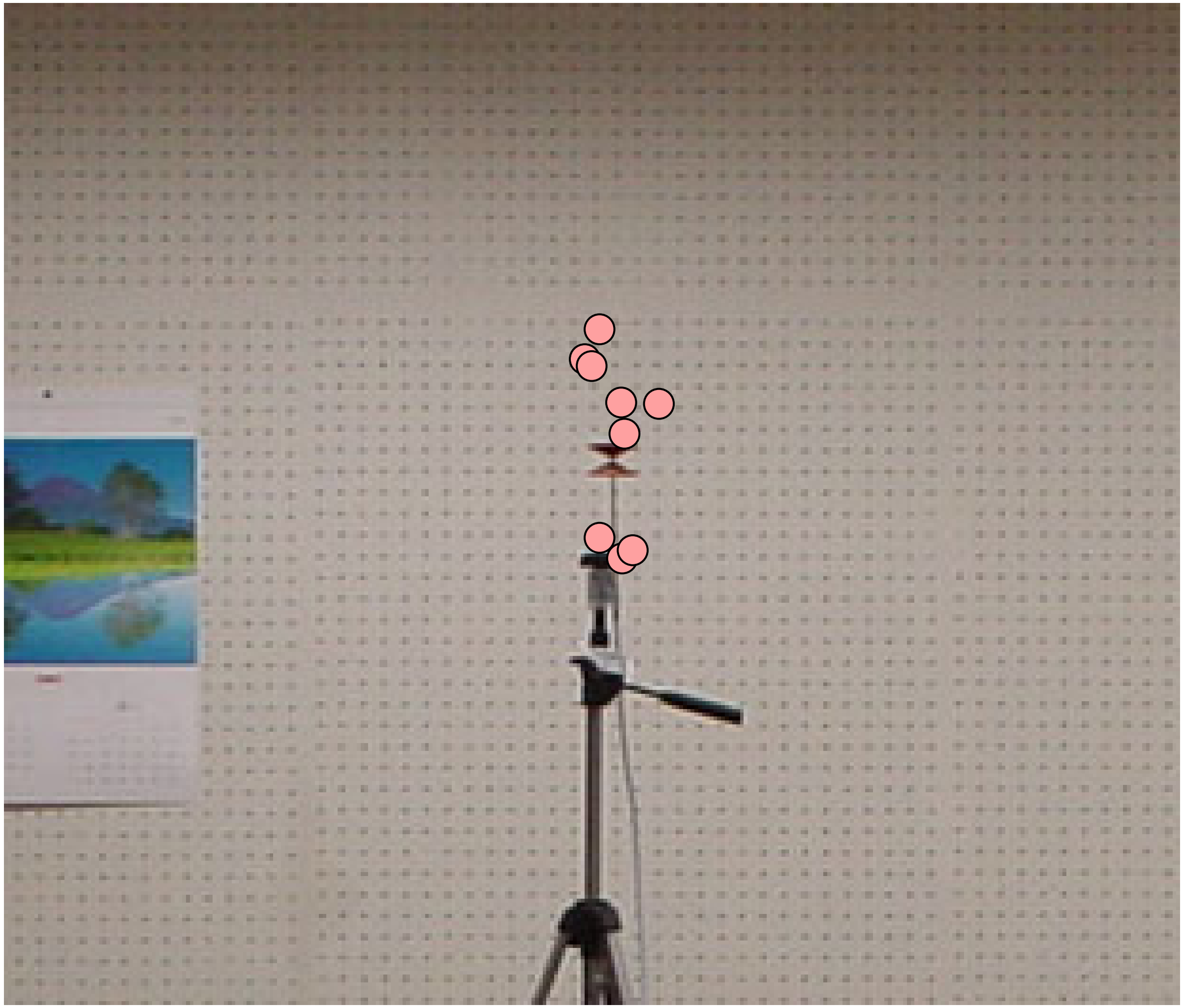

Maximum deviation is 17cm from source point.

Estimated by measurement

Measurement Result (6)

- Estimated reflection points in back wall reflection

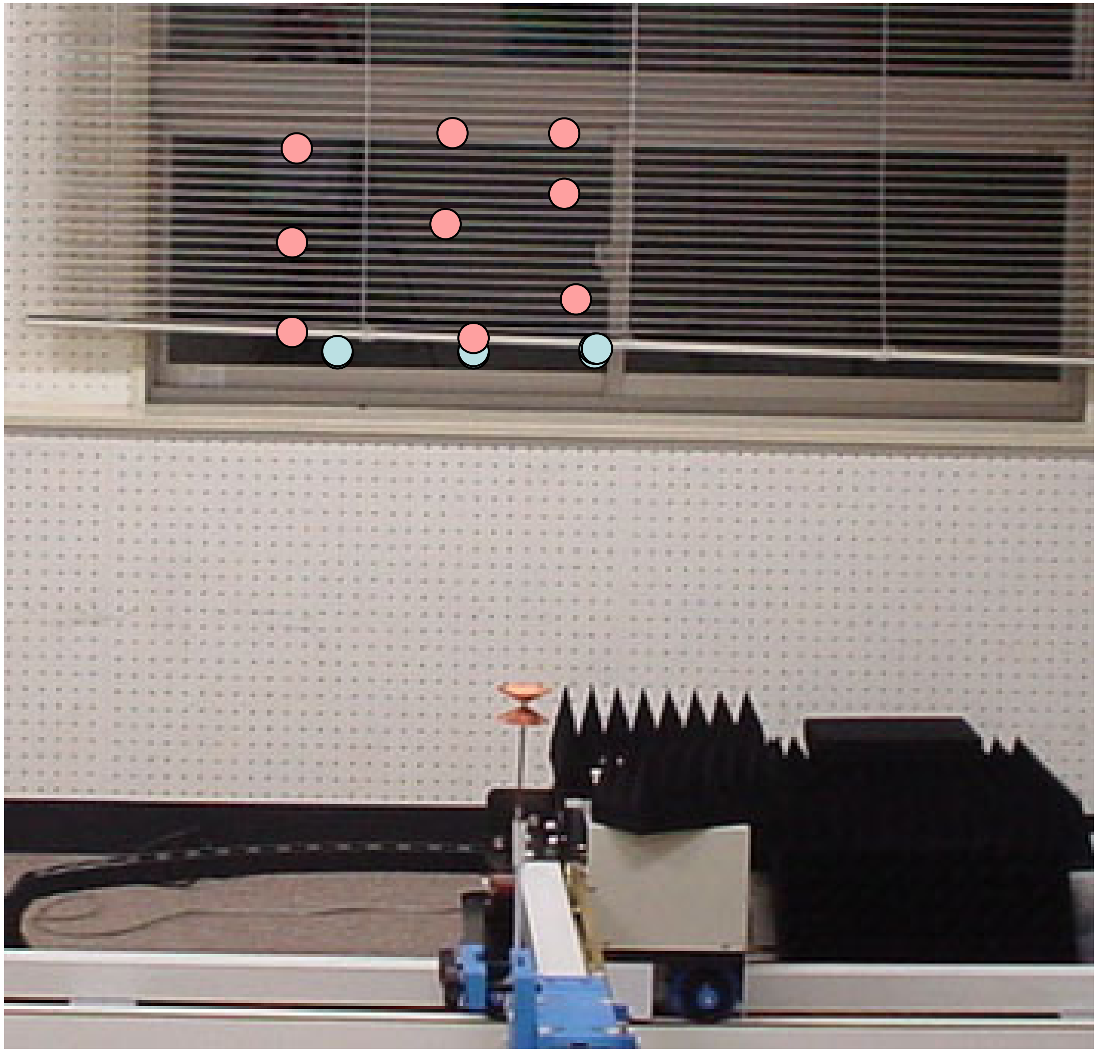

All the reflection points are above those predicted by GO.

Predicted by GO

Estimated by measurement

Discussion

- Some problems have been appeared.
  - 2 ~ 4 spurious waves detected during the estimation of 6 waves
  - Residual components after removing dominant paths
  - Signal model error (plane or spherical)
  - Estimation error based on inherent resolution of the algorithm implementation
  - Many distributed source points (diffuse scattering)

➡ Further investigation in simple environment

Performance Evaluation in Anechoic Chamber

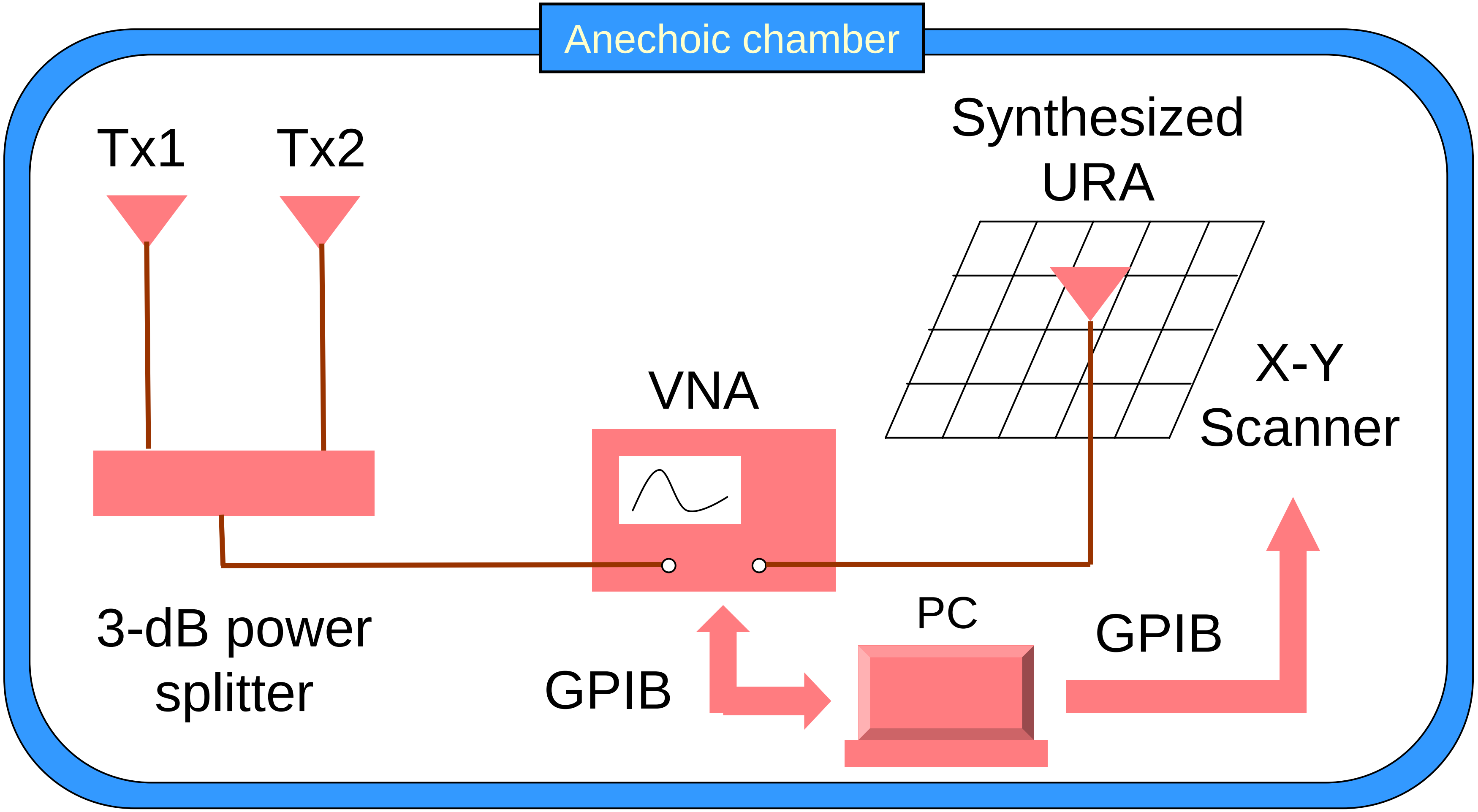

Specifications of Experiment

- Frequency : 3.1 ~ 10.6 GHz
  - 0.13 ns Fourier resolution
- Antenna scanning plane : 432 mm square in horizontal plane
  - 10 deg Fourier resolution
  - 48 mm element spacing
    (less than half wavelength @ 3.1 GHz)
- Wideband monopole antennas were used
  - Variation of group delay < 0.1 ns within the considered bandwidth
- SNR at receiver : About 25 dB

Aim of Anechoic Chamber Test

- Evaluation of spatio-temporal resolution
  - Separation and detection of two waves that
    - Spatially 10 deg different and same DT
    - Temporally 0.67 ns (= 20 cm) different and same DoA

Setup of Experiment

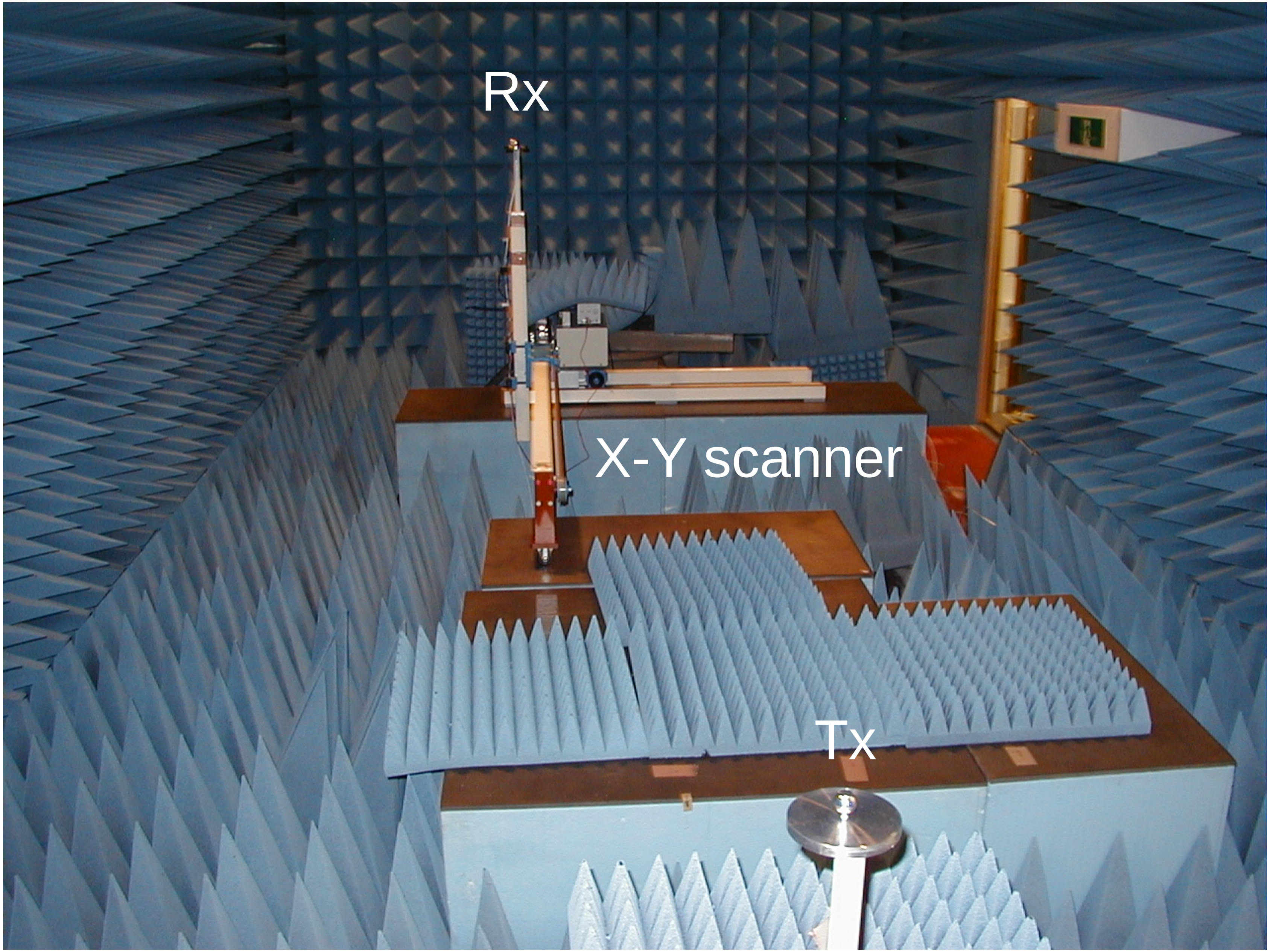

Spatial Resolution Test (1)

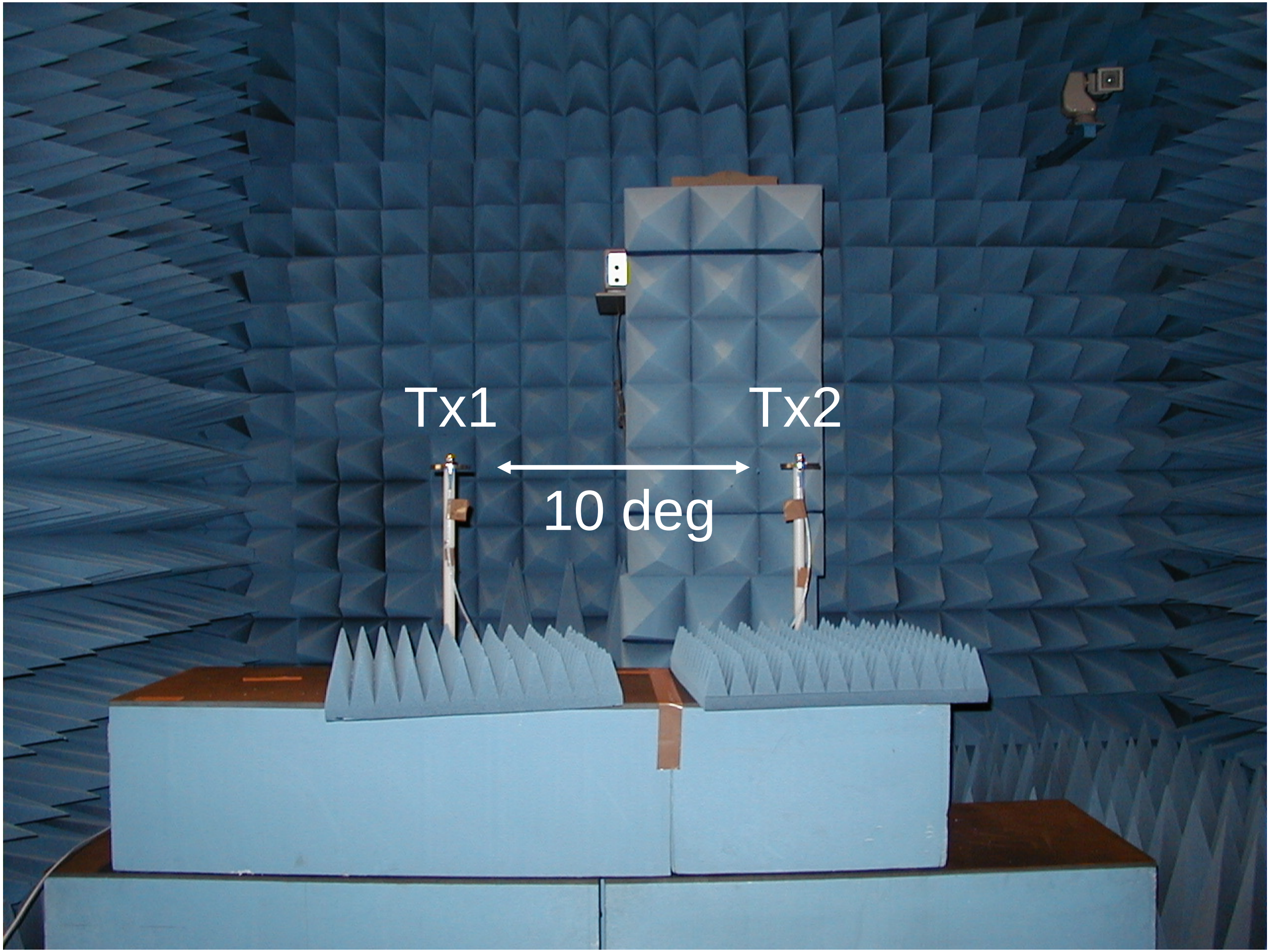

Spatial Resolution Test (2)

- 10 deg separated waves are accurately separated.
  - Parameters and spectra are accurately estimated.
  - The estimated phase denotes a deviation from free space phase rotation (~ 3 mm).
  - Antenna characteristics are already deconvolved.

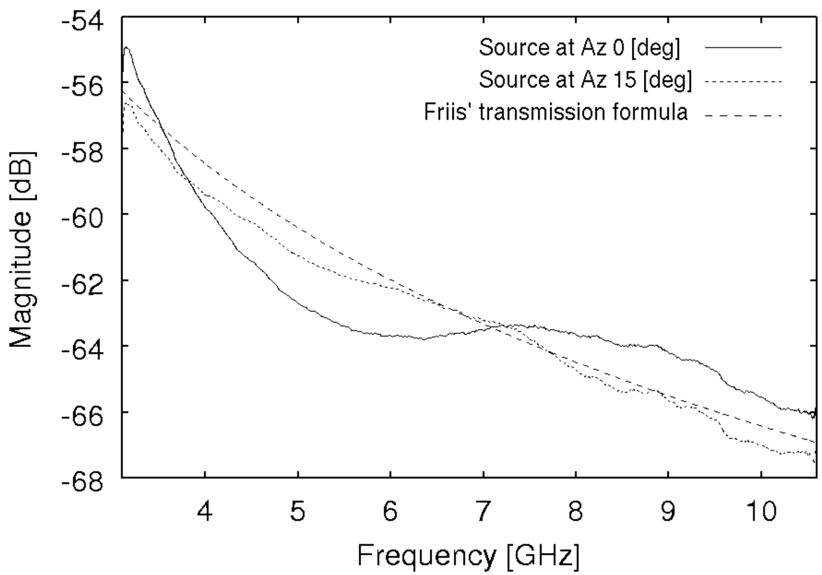

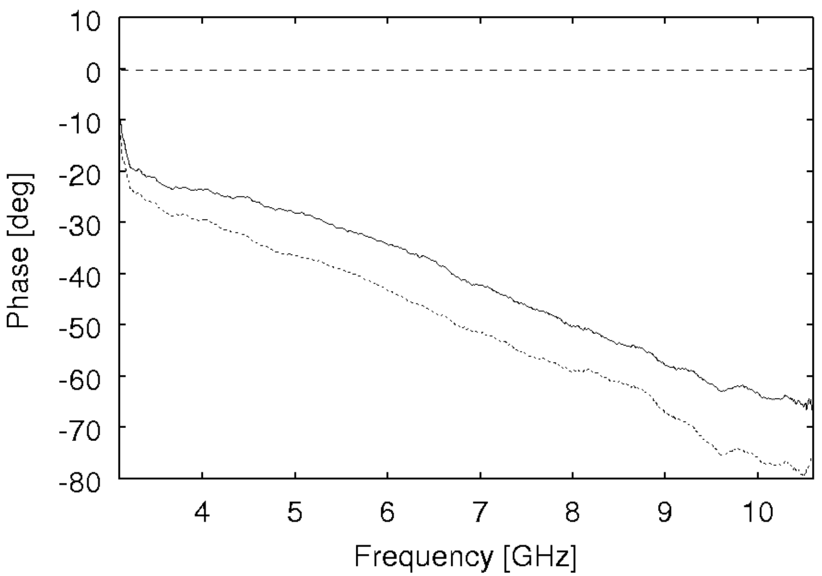

Temporal Resolution Test (1)

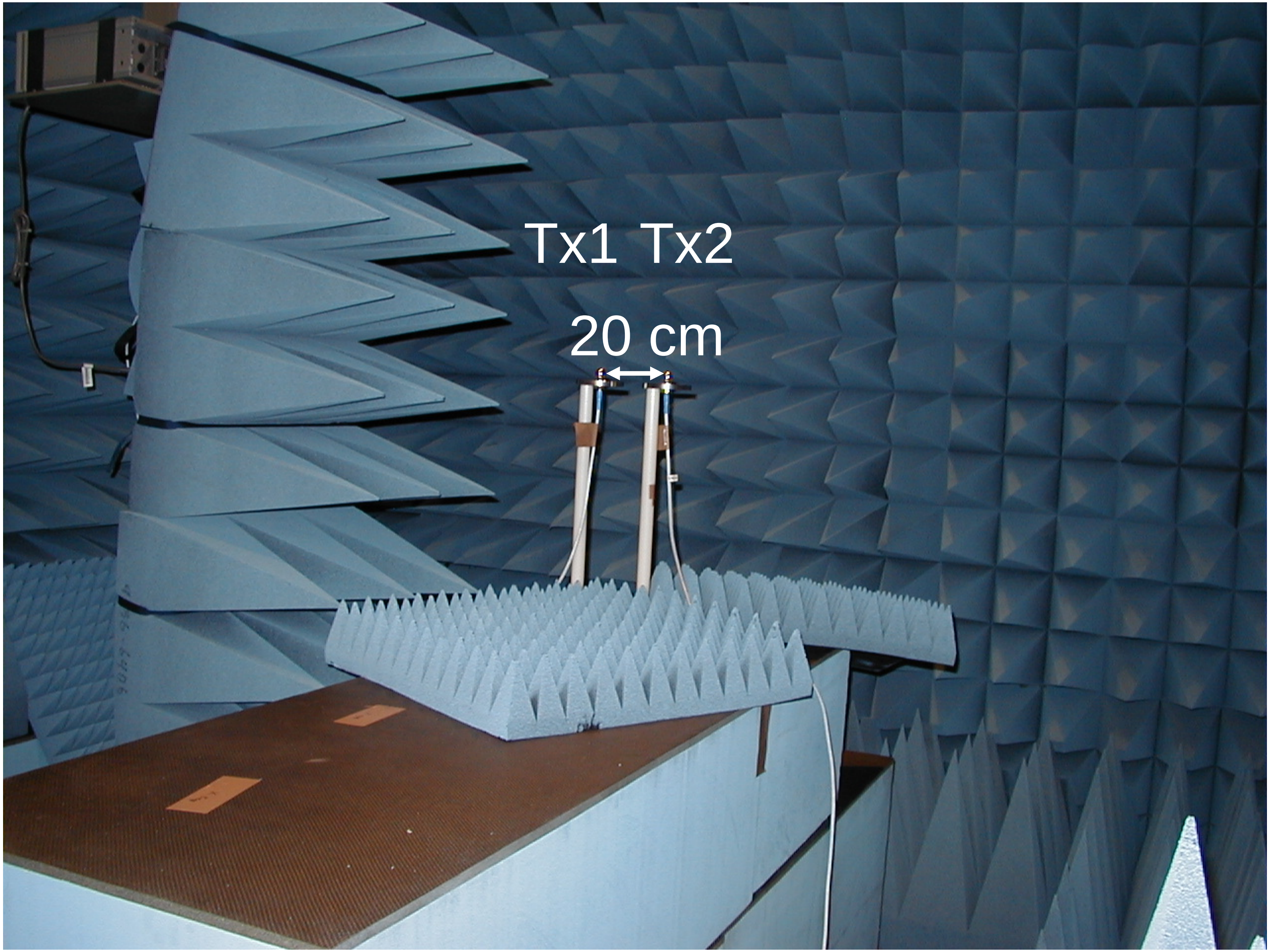

Temporal Resolution Test (2)

- 0.67 ns separated waves are accurately resolved.
  - Subband width : 1.5 GHz
  - Spectrum estimation is impossible in the higher and lower frequency region of

$$\left(\frac{1}{\Delta\tau = 0.67\,[\mathrm{ns}]}\right)\Big/2$$

$$= 0.75\,[\mathrm{GHz}]$$

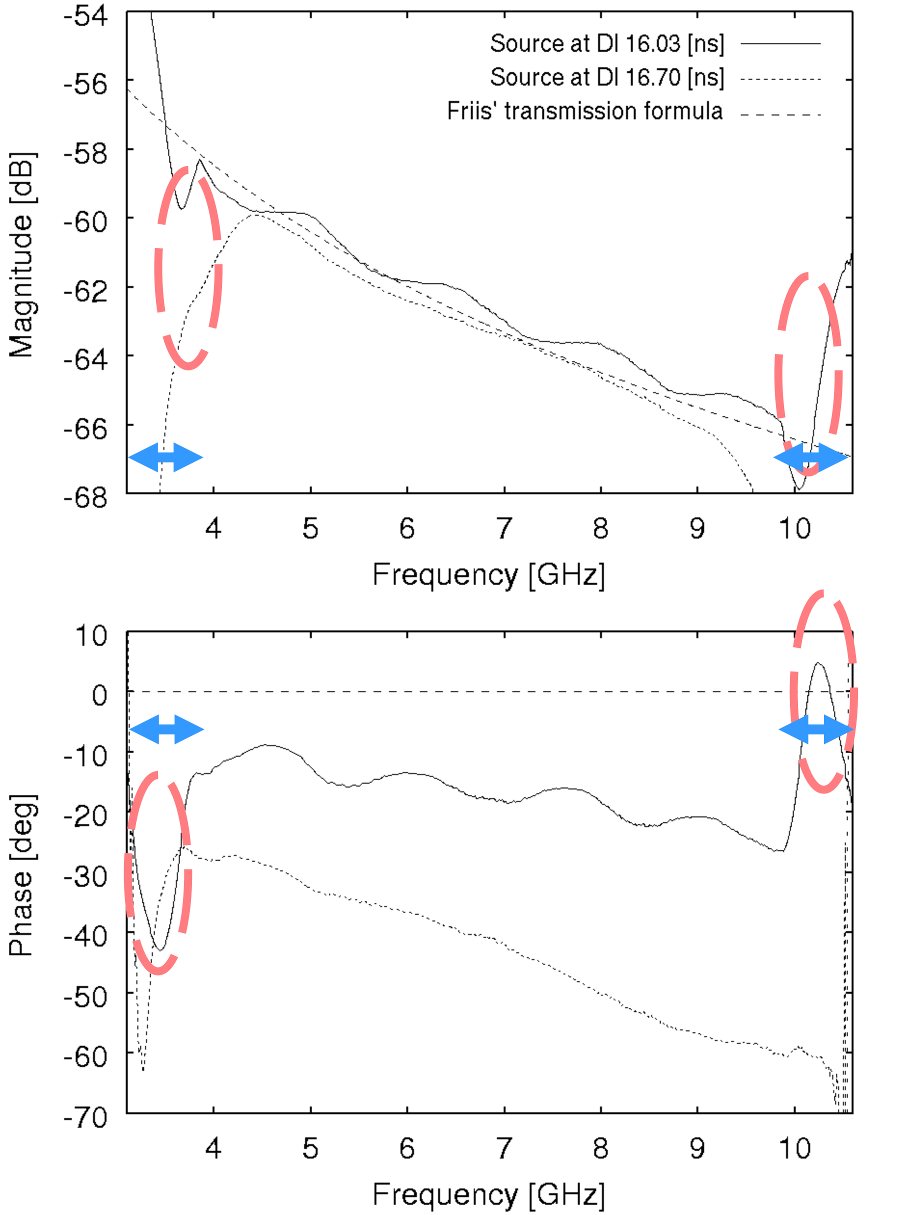

Subband Processing (1)

- … relieves a bias of parameter estimation due to amplitude and phase fluctuation within the band
- Tradeoff between the resolution and accuracy of parameter estimation: some optimization is needed !!

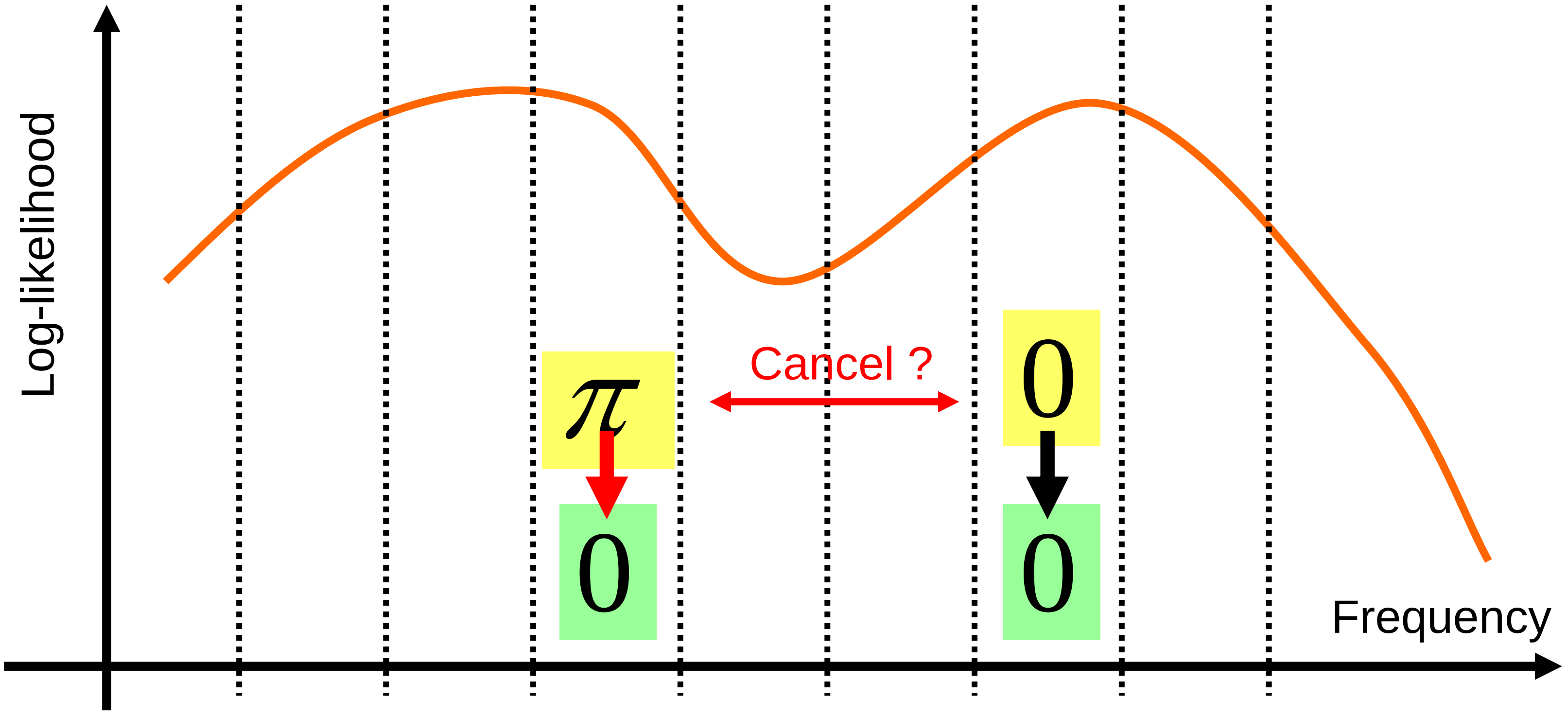

Subband Processing (2)

- How to choose the optimum bandwidth of subband?
  - Suppose two waves are $\Delta\theta$ and $\Delta\tau$ separated

		Angle resolution : θ_{res}	
		$\theta_{\text{res}} < \Delta\theta$	$\theta_{\text{res}} > \Delta\theta$
Delay resolution τ_{res}	$\tau_{\text{res}} < \Delta\tau$	Bandwidth within which deviation of antennas and propagation characteristics is sufficiently small	$\approx \dfrac{1}{\Delta\tau}$
	$\tau_{\text{res}} > \Delta\tau$		Impossible to resolve

Subband Processing (3)

- Behavior for the detection of two waves closer than the inherent resolution of the algorithm
  - Regard two waves as one wave (ex. same incident angle)
  - Two separated waves, but biased estimation of power (ex. 5 deg different incident angles)

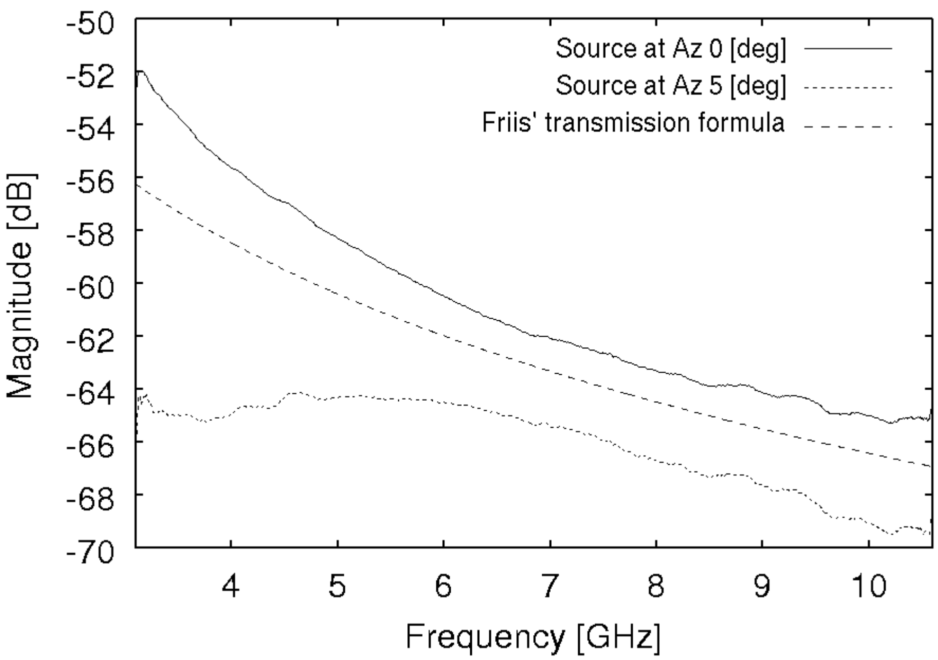

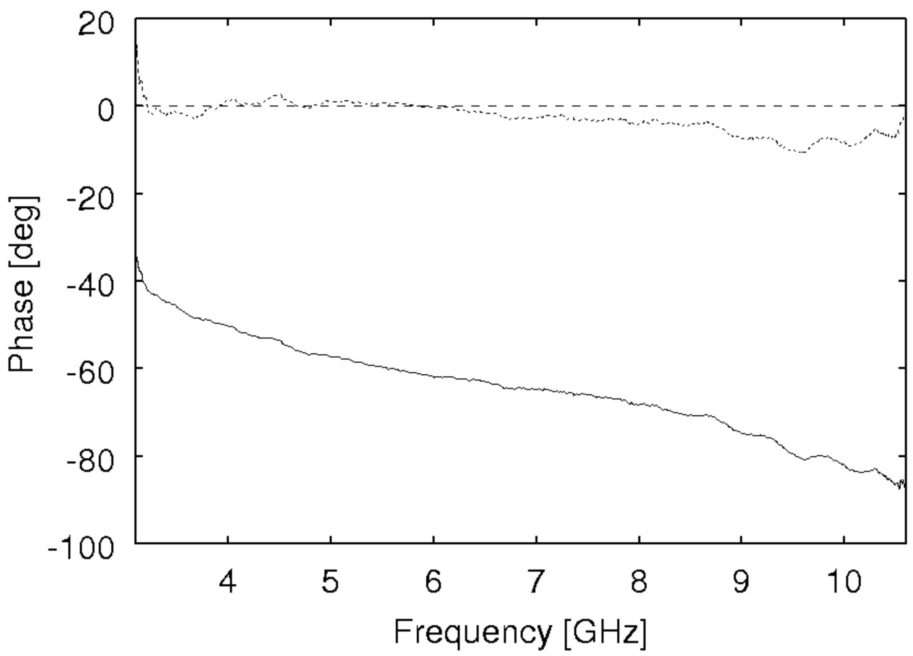

Deconvolution of Antenna Patterns

- Deconvolution of antennas
  - Construction of channel models independent of antenna type and antenna configuration
  - Deconvolution is post-processing (from the estimated spectrum by SAGE)
    - Simple implementation rather than the deconvolution during the search

Spherical vs Plane Wave Models (1)

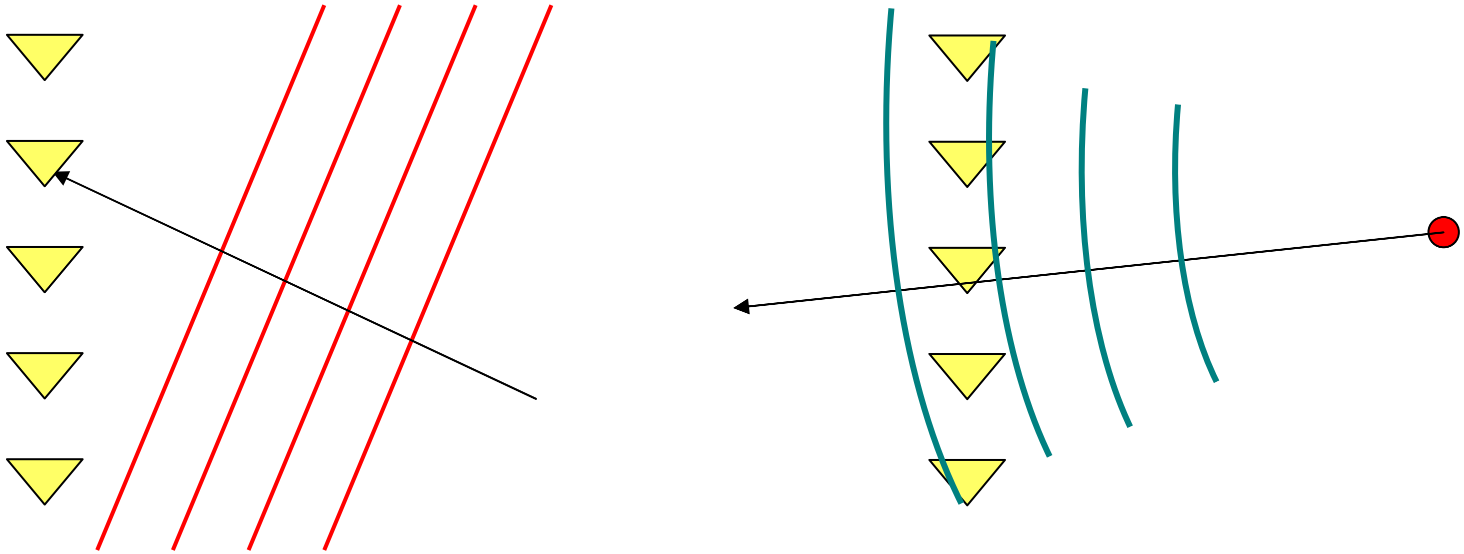

Plane wave incidence
(far field incidence)

Spherical wave incidence
(radiation from point source)

- How these models affect for the accurate estimation?
  - Spurious (ghost path) and detection of weak paths
  - Empirical evaluation of model accuracy

Spherical vs Plane Wave Models (2)

- Detection of 20 dB different two waves
  - Is a weaker source correctly detected?

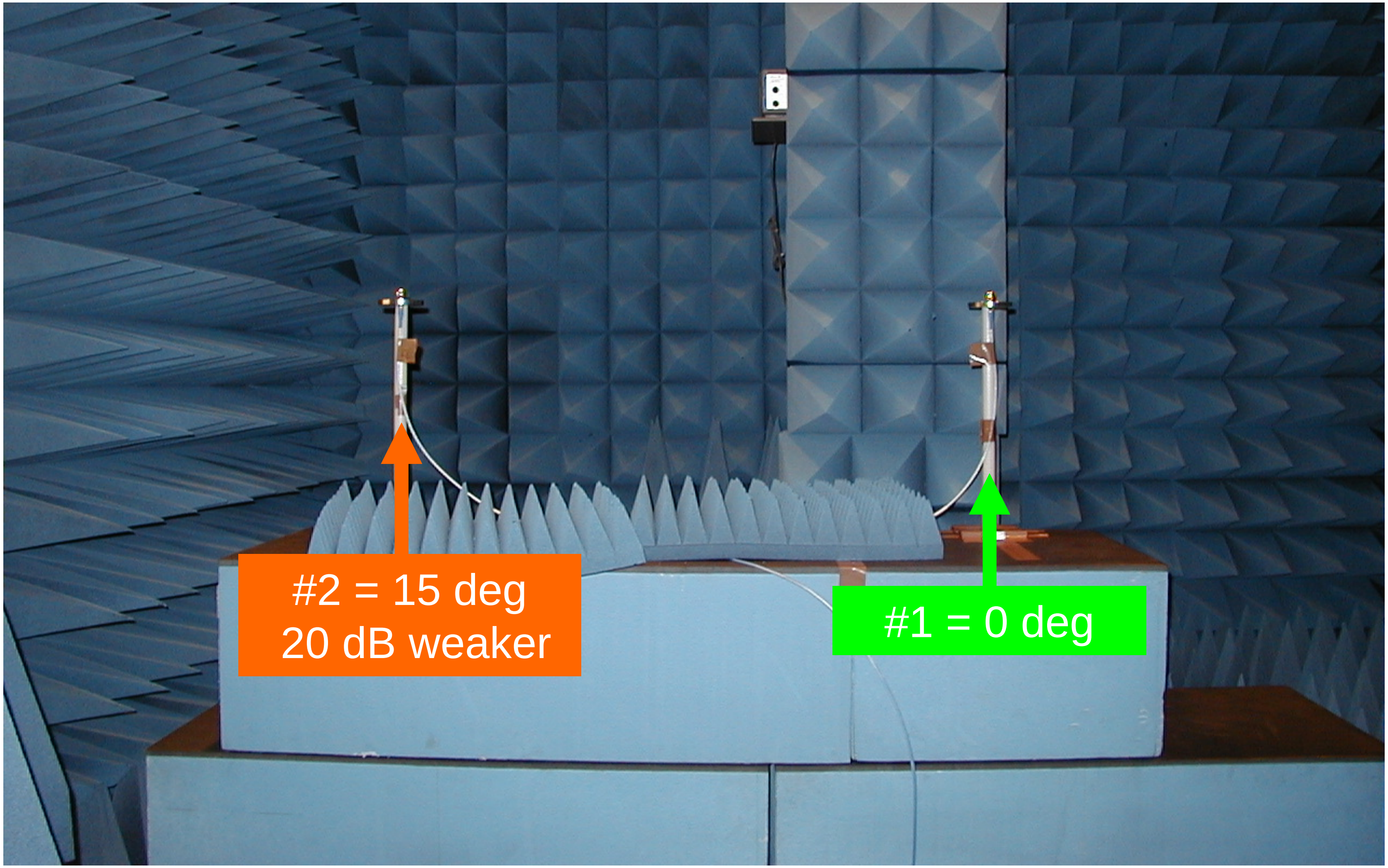

Spherical vs Plane Wave Models (3)

- Log-likelihood spectrum in the detection of weaker path

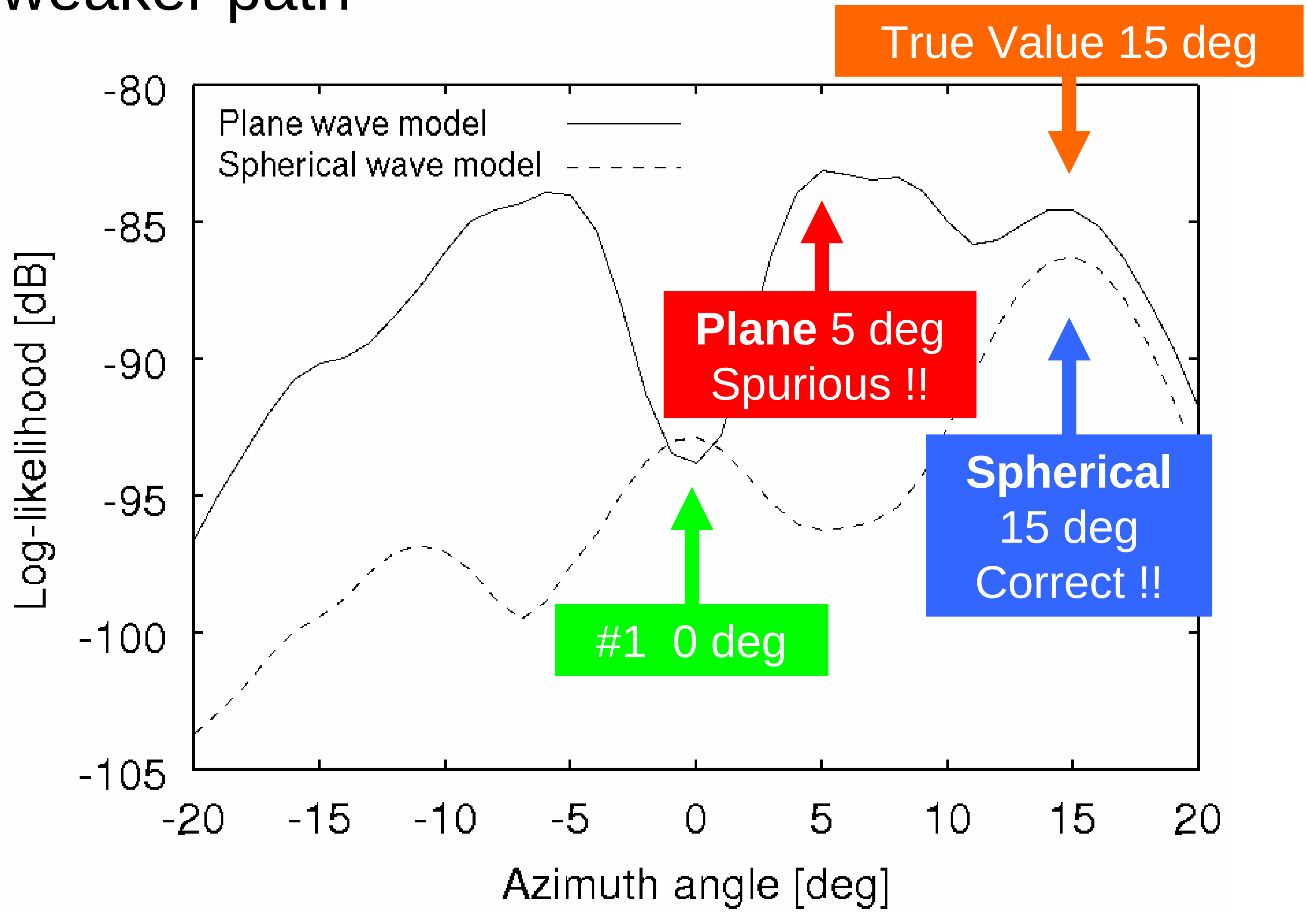

Summary of Evaluation Works (1)

- Evaluation of the proposed UWB channel sounding system in an anechoic chamber
  - Resolved spatially 10 deg, temporally 0.67 ns separated waves
  - Spectrum estimation is partly impossible in the highest and lowest frequency regions of $\frac{1}{2\Delta\tau}$.
  - The algorithm treats two waves closer than inherent resolution as one wave, or results in biased power estimation even if they are separated.

Summary of Evaluation Works (2)

- For reliable UWB channel estimation with SAGE algorithm
  - An optimum way to choose the bandwidth of subband
  - The number of waves estimation is done by SIC- type procedure
- Deconvolution of antennas effects from the results of SAGE
  - For channel models independent of antennas

Summary of Evaluation Works (3)

- Spherical incident wave model is more robust than plane wave incident model
  - Spurious reduction is expected
  - Effective in the detection of weaker path

Indoor Double Directional Measurement (1)

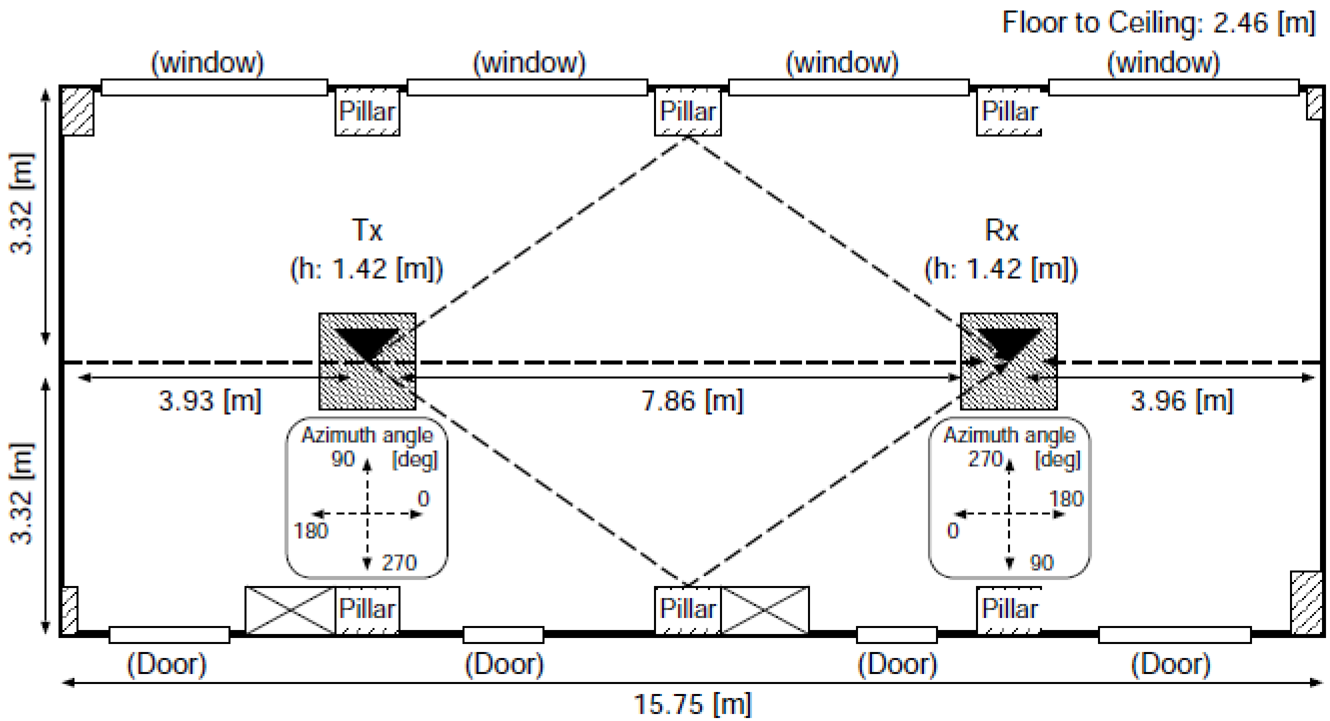

(a) Top view

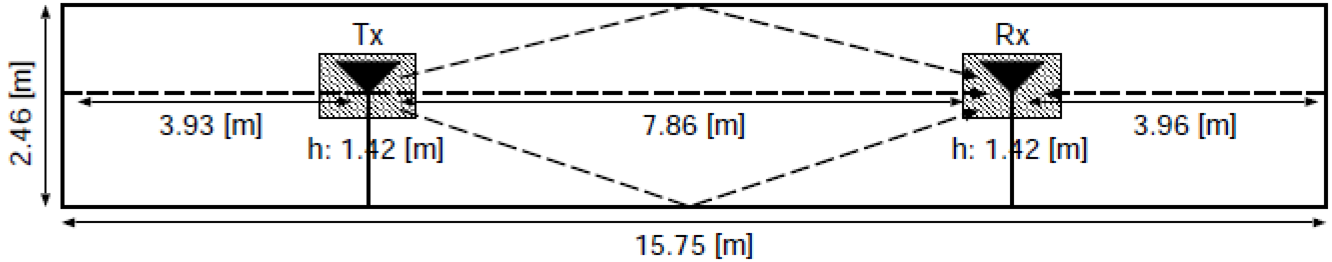

(b) Side view

Indoor Double Directional Measurement (2)

Azimuth-Delay spectrum

Tx side

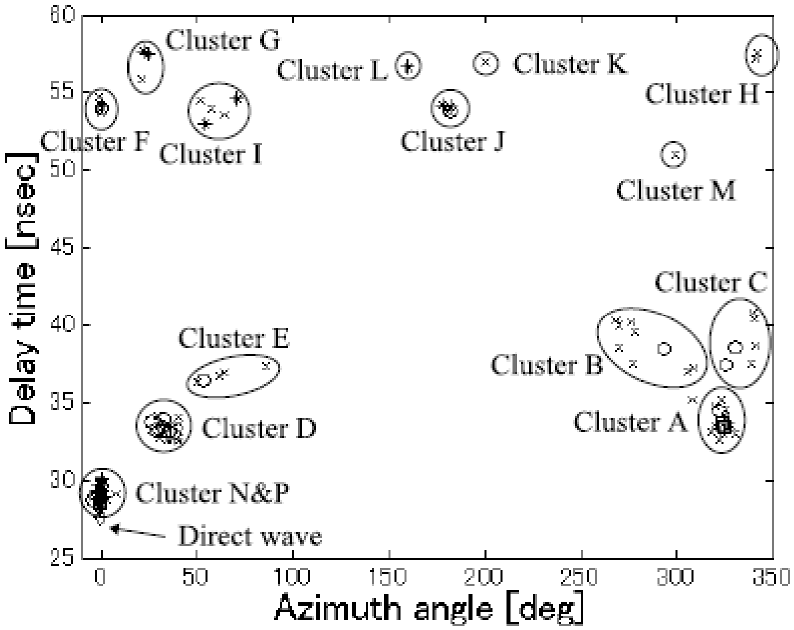

Rx side

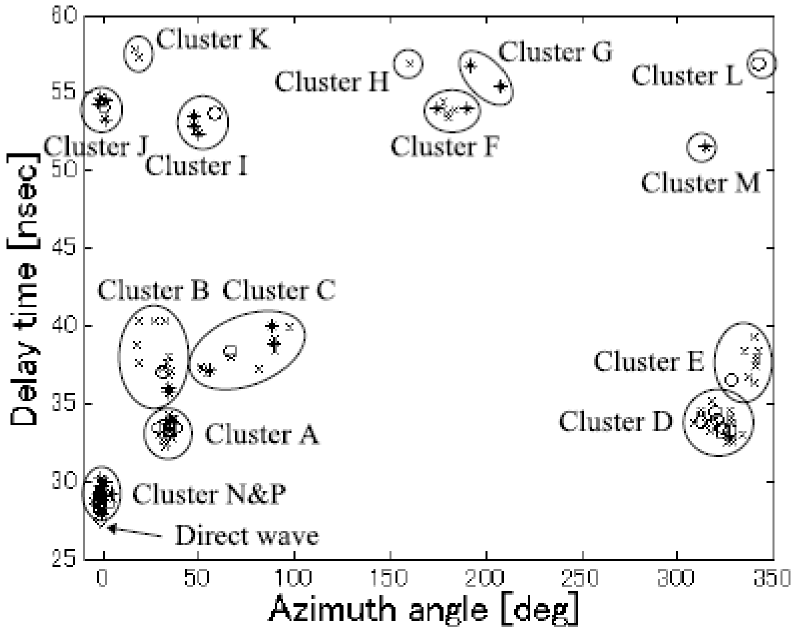

Above -80 [dB] ◇ -80 to -90 [dB] □ -90 to -100 [dB] ○
-100 to -110 [dB] × Below -110 [dB] *

Indoor Double Directional Measurement (3)

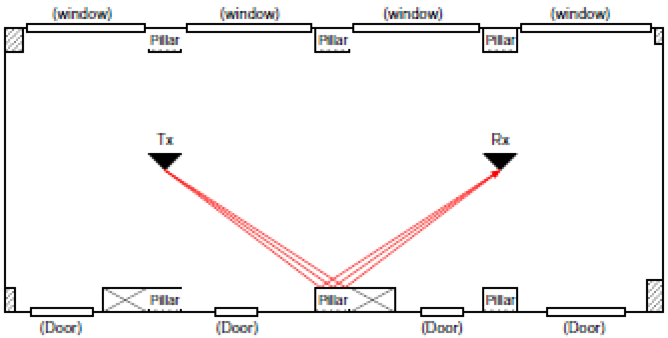

(a) Cluster A

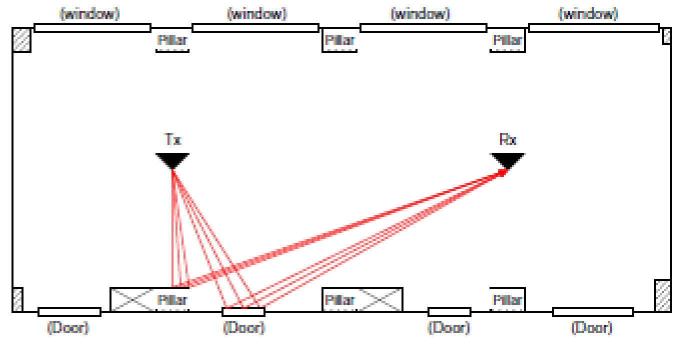

(b) Cluster B

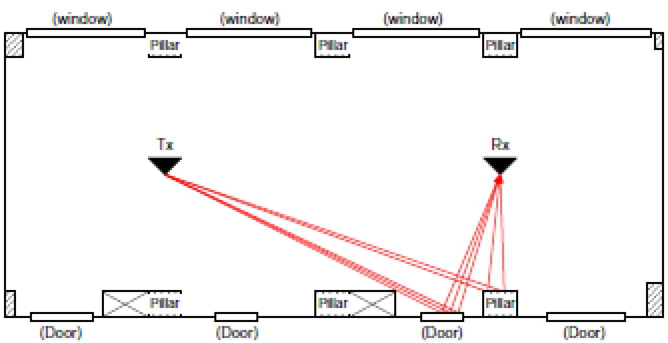

(c) Cluster C

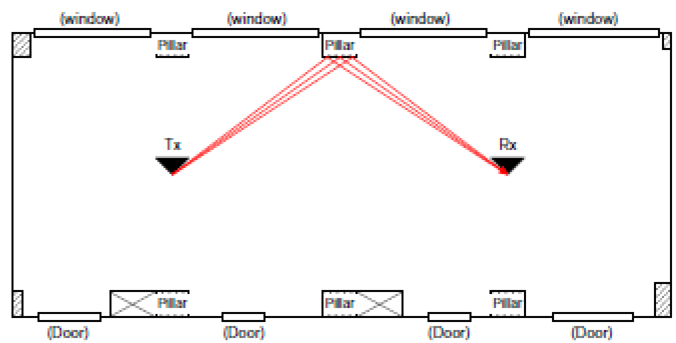

(d) Cluster D

Indoor Double Directional Measurement (4)

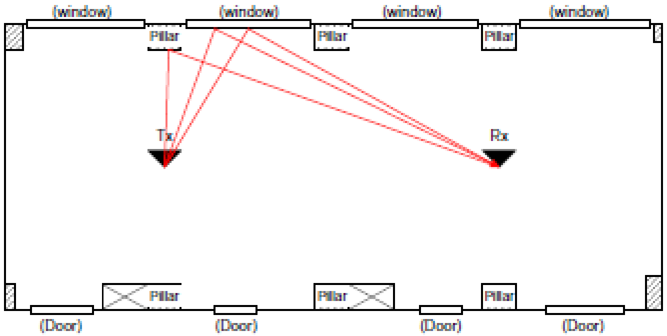

(e) Cluster E

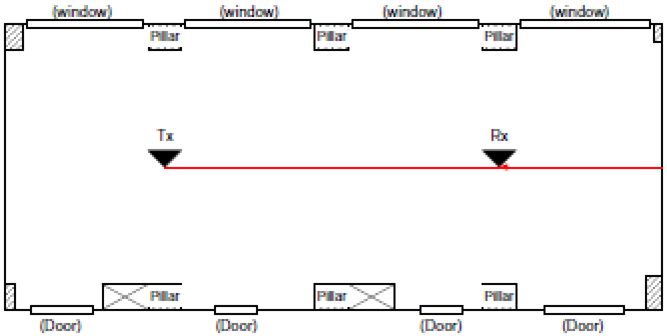

(f) Cluster F

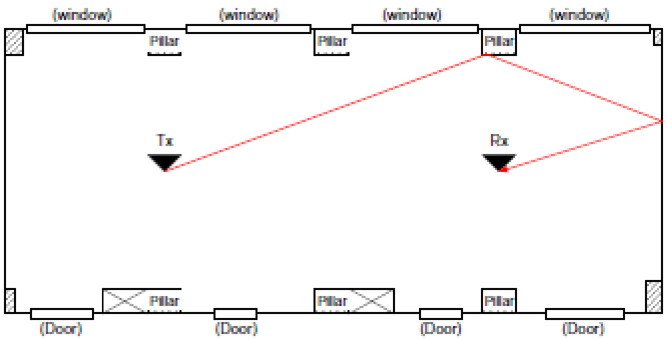

(g) Cluster G

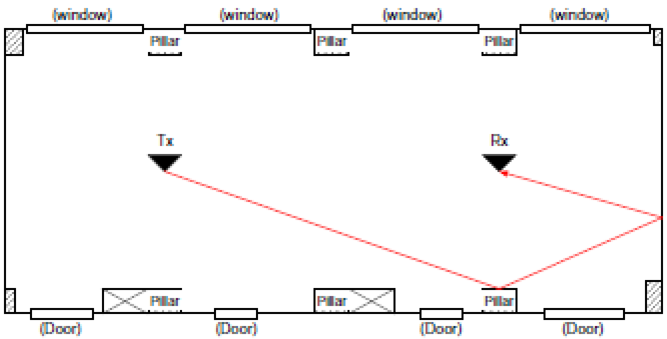

(h) Cluster H

Indoor Double Directional Measurement (5)

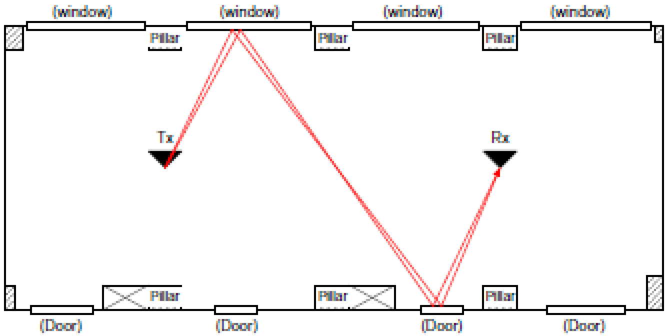

(i) Cluster I

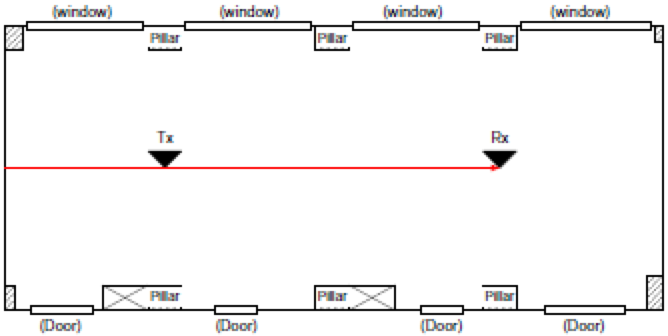

(j) Cluster J

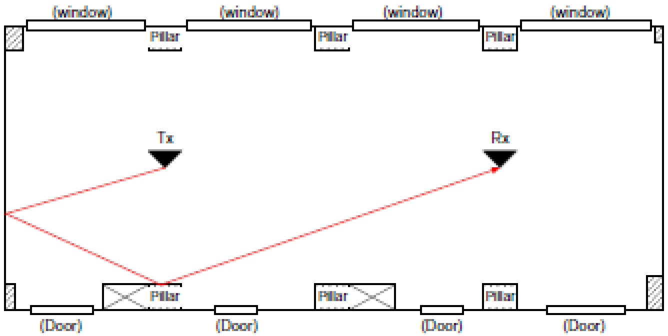

(k) Cluster K

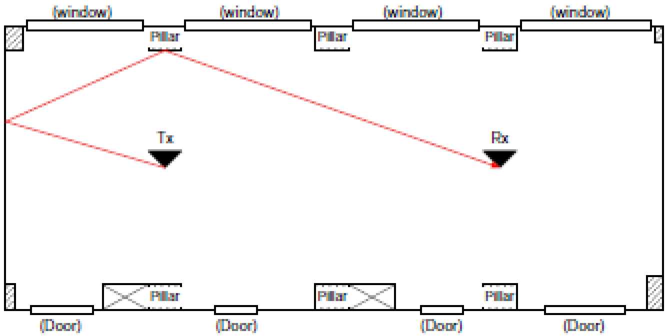

(l) Cluster L

Indoor Double Directional Measurement (6)

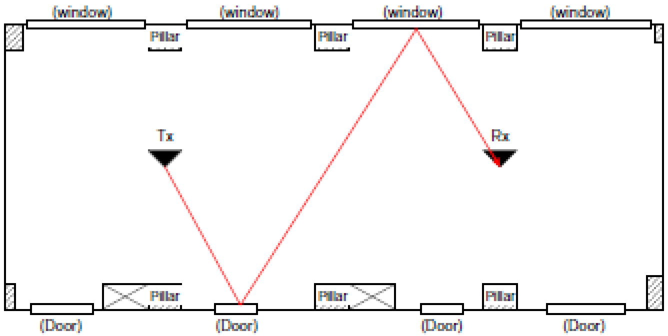

(m) Cluster M

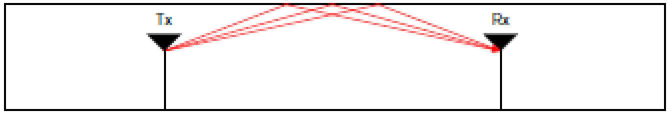

(n) Cluster N

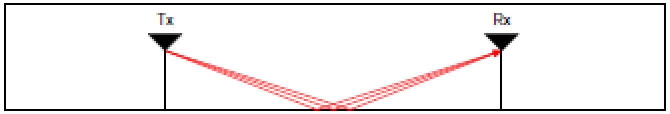

(p) Cluster P

Summary

- Background and motivation of double directional sounding
- Antennas and propagation in UWB
- UWB double directional channel sounding system
- Parametric multipath modeling for UWB
- ML-based parameter estimation
- Examples

References

- Jun-ichi Takada, Katsuyuki Haneda, and Hiroaki Tsuchiya, "Joint DOA/DOD/DTOA estimation system for UWB double directional channel modeling," to be published in S. Chandran (eds), "Advances in Direction of Arrival Estimation," to be published from Artech House, Norwood, MA, USA.
- Katsuyuki Haneda, Jun-ichi Takada, and Takehiko Kobayashi, "Experimental Evaluation of a SAGE Algorithm for Ultra Wideband Channel Sounding in an Anechoic Chamber," joint UWBST & IWUWBS 2004 International Workshop on Ultra Wideband Systems Joint with Conference on Ultra Wideband Systems and Technologies (Joint UWBST & IWUWBS 2004), May 2004 (Kyoto, Japan).
- Hiroaki Tsuchiya, Katsuyuki Haneda, and Jun-ichi Takada, "UWB Indoor Double-Directional Channel Sounding for Understanding the Microscopic Propagation Mechanisms," 7th International Symposium on Wireless Personal Multimedia Communications (WPMC 2004), pp. 95-99, Sept. 2004 (Abano Terme, Italy).